Supplementary information for:

A rapidly closing window for coral persistence under global warming

Yves-Marie Bozec*, Arne A.S. Adam, Beatriz Arellano Nava, Anna K. Cresswell, Vanessa Haller-Bull, Takuya Iwanaga, Liam Lachs, Samuel A. Matthews, Jennifer K. McWhorter, Kenneth R.N. Anthony, Scott A. Condie, Paul R. Halloran, Juan-Carlos Ortiz, Cynthia Riginos, Peter J. Mumby.

* Corresponding author. Email: y.bozec@uq.edu.au

Contents:

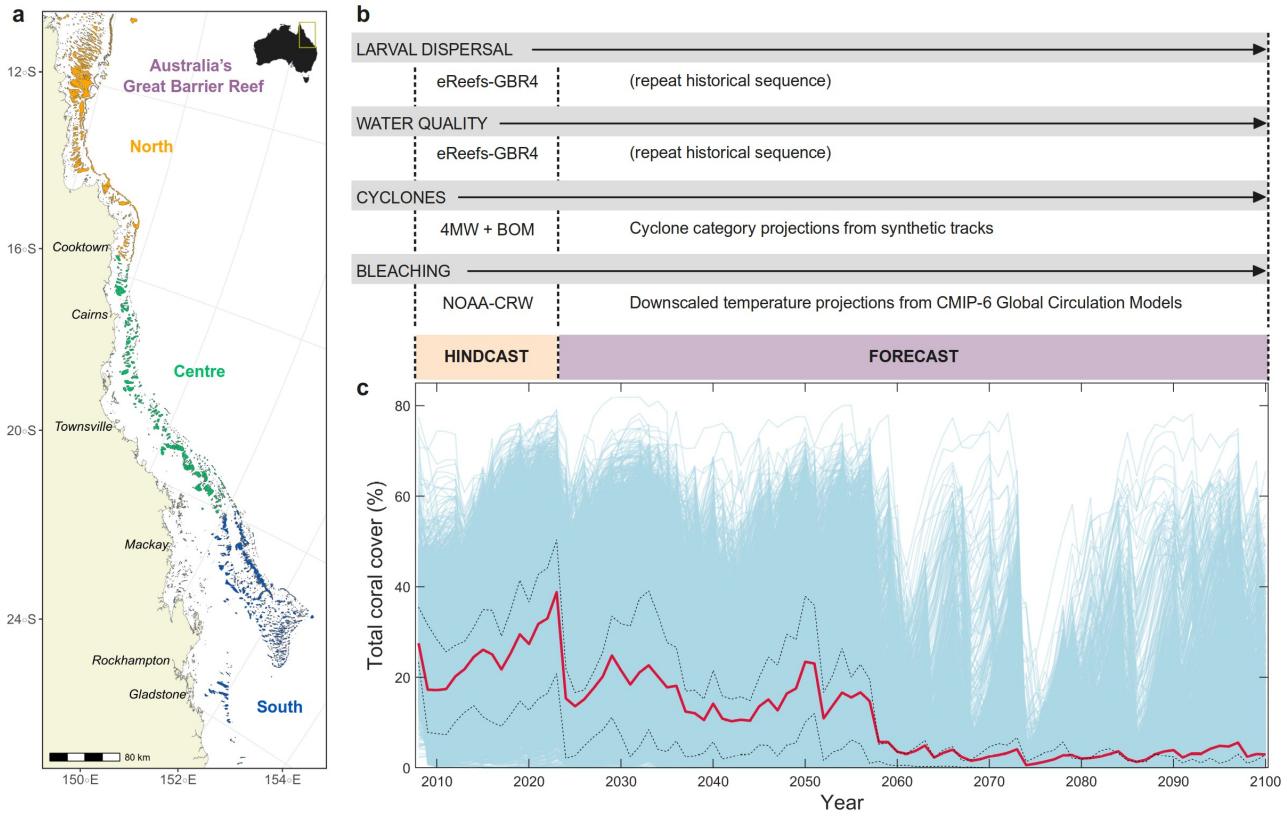

Supplementary Fig. 1. Model domain, reef definition and environmental forcing. a Spatial domain of ReefMod-GBR consisting in 3,806 individual reefs distributed along Australia's Great Barrier Reef (GBR). Reef polygons mapped using the geospatial data 'Great Barrier Reef Features (GDA94)' publicly available from the Reef Geohub platform (https://reef-geohub-ext-geohubgbrmpa.hub.arcgis.com/) **b** Environmental drivers of coral metacommunity dynamics used for spatially-realistic reconstructions[1] (hindcast) and future projections (forecast). Coral and CoTS larval connectivity is derived from biophysical simulations performed over six spawning seasons[2,3] using a three-dimensional hydrodynamic model of the GBR[4] at 4-km resolution (eReefs-GBR4). Water quality is represented by suspended sediment and chlorophyll concentrations inferred from eReefs-GBR4 coupled hydrodynamic-biogeochemical simulations[4,5]. Past exposure to cyclones is reconstructed from hindcast predictions of damaging wave height using the 4MW model[6] paired with estimates of cyclone category inferred from historical tracks[1] of the Australian Tropical Cyclone Database[7] maintained by the Australian Bureau of Meteorology (BOM). Forward projections of cyclone categories are sampled from a library of synthetic cyclone tracks for the GBR[8]. Historical heat stress is determined from satellite-derived records of maximum annual Degree Heating Week (DHW) provided at 5-km resolution by NOAA Coral Reef Watch[9] (CRW). Future heat stress is based on sea surface temperature projections from climate models of the Coupled Model Intercomparison Project Phase 6 (CMIP6), further downscaled at 10-km resolution. **c** A single realisation of the combined hindcast and forecast projections of total coral cover across the GBR, illustrating the variability of coral cover trajectories among individual reefs (blue lines, n = 3,806). The red line indicates the average coral cover weighted by the area of each reef. The dashed lines represent the 25th and 75th percentiles of the yearly distribution of coral cover across all simulated reefs. Here, forecast projections were derived from one scenario of future cyclones and one scenario of future heat stress from the climate model CNRM-ESM2-1 (Supplementary Table 1) under the emissions scenario (Shared Socioeconomic Pathway, SSP) SSP2-4.5.

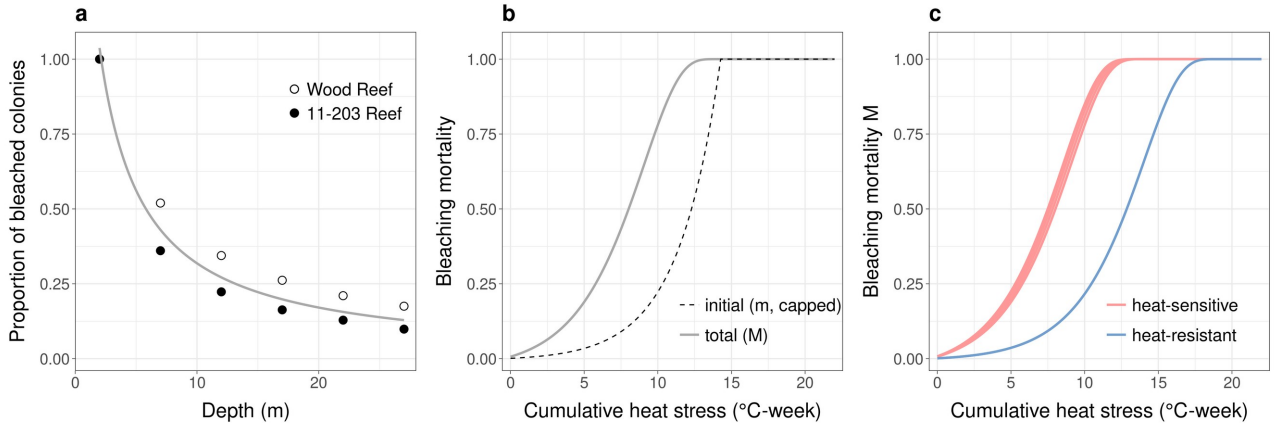

Supplementary Fig. 2. Modelling of bleaching-induced coral mortality. a Modelling of bleaching prevalence along a depth profile of light attenuation as observed in the Northern GBR four weeks after the peak of the 2016 mass-bleaching event[10]. Bleaching prevalence measured at Wood Reef (DHW = 9.0 °C-week) and at 11-203 Reef (DHW = 5.8 °C-week) was re-expressed as the proportion of bleached colonies relative to that observed at 2 m depth and fitted with a linear model after an inverse transformation ($R^2 = 0.78$). **b** Empirical relationship between cumulative heat stress (DHW) and initial mortality (*m*, Eq. 1) and the resulting long-term, total mortality (*M*, Eq. 3) for corymbose acroporids extrapolated at 7 m depth. **c** Simulated total mortality along a gradient of DHW at 7 m depth for the six coral groups, showing differences among taxa due to variable susceptibilities to bleaching (sensitivity coefficient *s* in Eq. 1). For the three acroporid groups and the group of pocilloporids (heat-sensitive taxa, red curves), *s* was set to 1.5, 1.6, 1.4, and 1.7, respectively. For submassive/encrusting corals and large massive corals (heat-tolerant taxa, blue curves), *s* was set to 0.25. Sensitivity coefficients were determined based on taxon-specific mortality observed on the GBR at the peak of the 2016 mass bleaching[11].

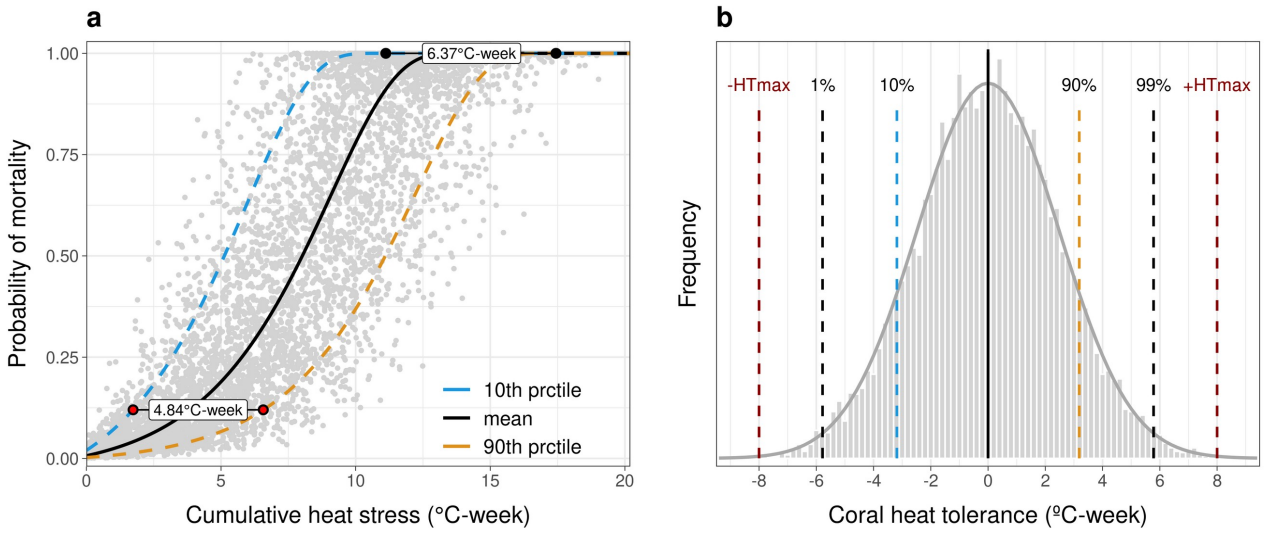

Supplementary Fig. 3. Modelling heat tolerance variability across coral colonies. a Simulated mortality for 10,000 virtual colonies of corymbose acroporids (grey dots) for randomly generated values of cumulative heat stress (DHW). Each coral was assigned with a heat tolerance (HT) value (ºC-week) generated at random from an initial normal distribution of mean $\mu = 0$ and standard deviation sd = 2.49 (thermally naive distribution). The blue and orange DHW-mortality curves indicate, respectively, the bleaching response of the 10th and 90th percentiles of this distribution, which reproduce a difference of 4.84 ºC-week inferred at the cut-off mortality of 12% (red dots) among samples of *Acropora digitifera* under experimental heat stress as reported in ref. 12. The maximum difference (6.37 ºC-week) is achieved at 100% mortality (black dots). **b** Normal distribution of HT values of corals within each of the six modelled groups at initialisation (grey curve) with one possible realisation (grey histogram bars, n = 10,000 coral colonies). Dotted lines indicate key percentiles, with the 10th and 90th corresponding to the experimental distribution of HT values[12] extrapolated at 100% mortality. Red dotted lines indicate the assumed hard evolutionary limits of heat tolerance ($\pm HT_{max} = 8$ ºC-week), which bound the generation of HT values for any newly generated coral. A coral with a HT of 0 ºC-week (mean of the HT distribution, black line) has a mortality that follows the mean bleaching response of the group at initialisation (black curve in **a**).

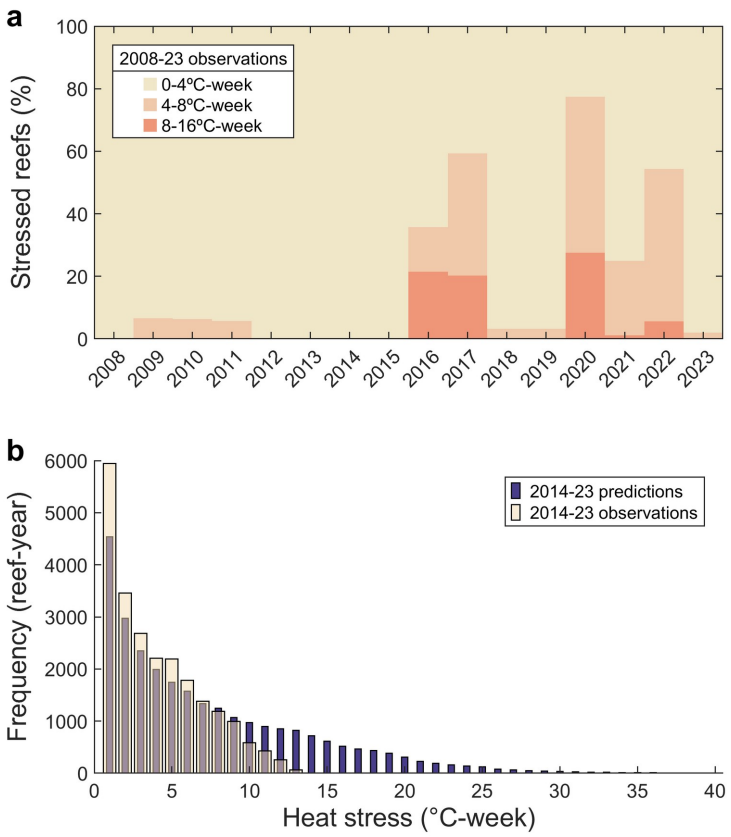

Supplementary Fig. 4. Recent heat stress on the Great Barrier Reef. a Proportion of individual reefs (n = 3,806) under different categories of heat stress (DHW; °C-week) from 2008 to 2023 derived from 5-km resolution satellite observations of sea-surface temperatures (NOAA Coral Reef Watch[9]). **b** Comparison of satellite observations vs. CMIP6 model predictions of reef-level DHW between 2014–2023 (n = 3,806 reefs × 10 years). Predicted (i.e., hindcast) DHW frequencies were averaged across the ten CMIP6 climate models and the five SSPs using the Equilibrium Climate Sensitivities as weights (see Methods).

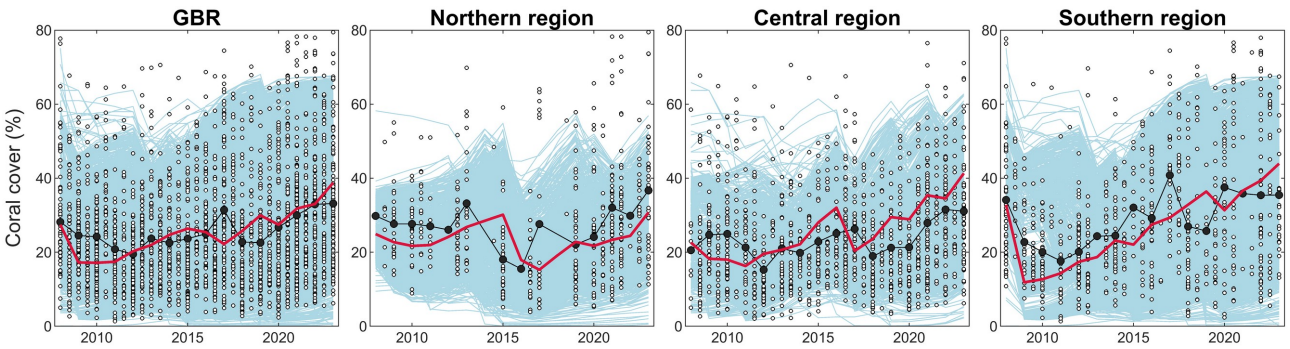

Supplementary Fig. 5. Hindcast (2008–2023) reconstruction of coral cover trajectories on the Great Barrier Reef. Trajectories of total coral cover (blue lines: individual reef predictions averaged over 20 simulations; red line: regional average) are represented for the entire GBR (n = 3,806 reefs) and for the northern (n = 1,201 reefs), central (n = 957 reefs) and southern (n = 1,648 reefs) regions. Data points represent coral cover observations derived from the Long-Term Monitoring Program of the Australian Institute of Marine Science[13] (photo-transect and manta tow estimates, further adjusted following ref. 1): open dots correspond to individual reef surveys and filled dots indicate the annual average across all surveys. Average coral cover was not calculated for years with fewer than five reef surveys. An annual model error was calculated as the difference between the predicted and observed mean coral cover for each available year between 2009 and 2023 (excluding the 2008 observations, which were used to initialise coral cover), resulting in a mean annual error, as percentage points, of −0.3% (95% central interval: −9.3 – 7.5%), −3.3% (−12.6 – 12.3%), +2.3% (−7.0 – 10.6%) and −2.1% (−11.6 – 10.8%) for the GBR, northern, central and southern reconstructions, respectively.

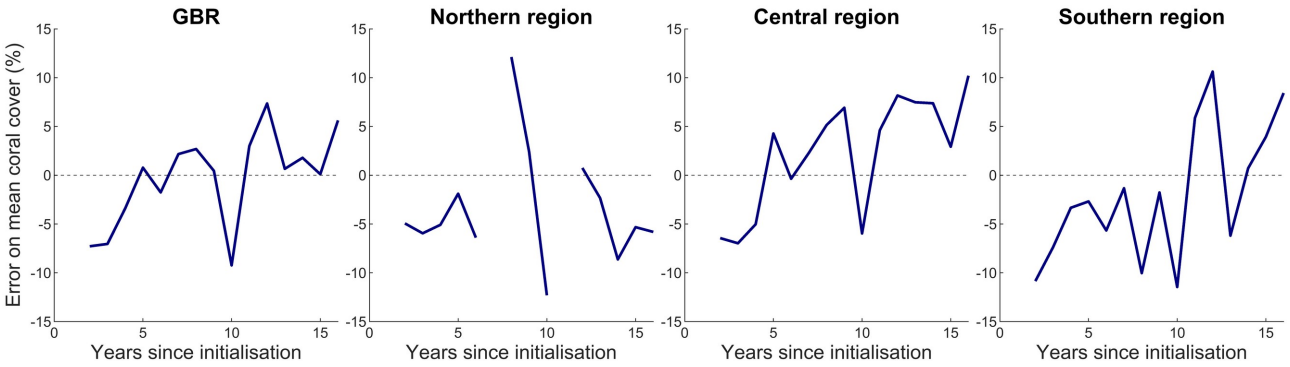

Supplementary Fig. 6. Annual model errors for the 2008–2023 reconstruction of mean coral cover. Model errors were calculated as the difference between predicted and observed mean coral cover (as shown in Supplementary Fig. 5), for each subsequent year after model initialisation in 2008. Errors were not computed when fewer than five reef observations were available, which occurred only in the Northern region. These discrepancies reveal fluctuating differences between model predictions and observations of coral cover throughout the hindcast period. Some of the largest discrepancies occurred in 2009, one year after initialisation, primarily due to incorrect estimates of reef-specific exposure to Tropical Cyclone Hamish. While such inaccuracies in environmental forcing affect the reconstruction of coral cover trajectories, they do not compromise the core assumptions underlying the simulation of coral demographics and adaptive responses.

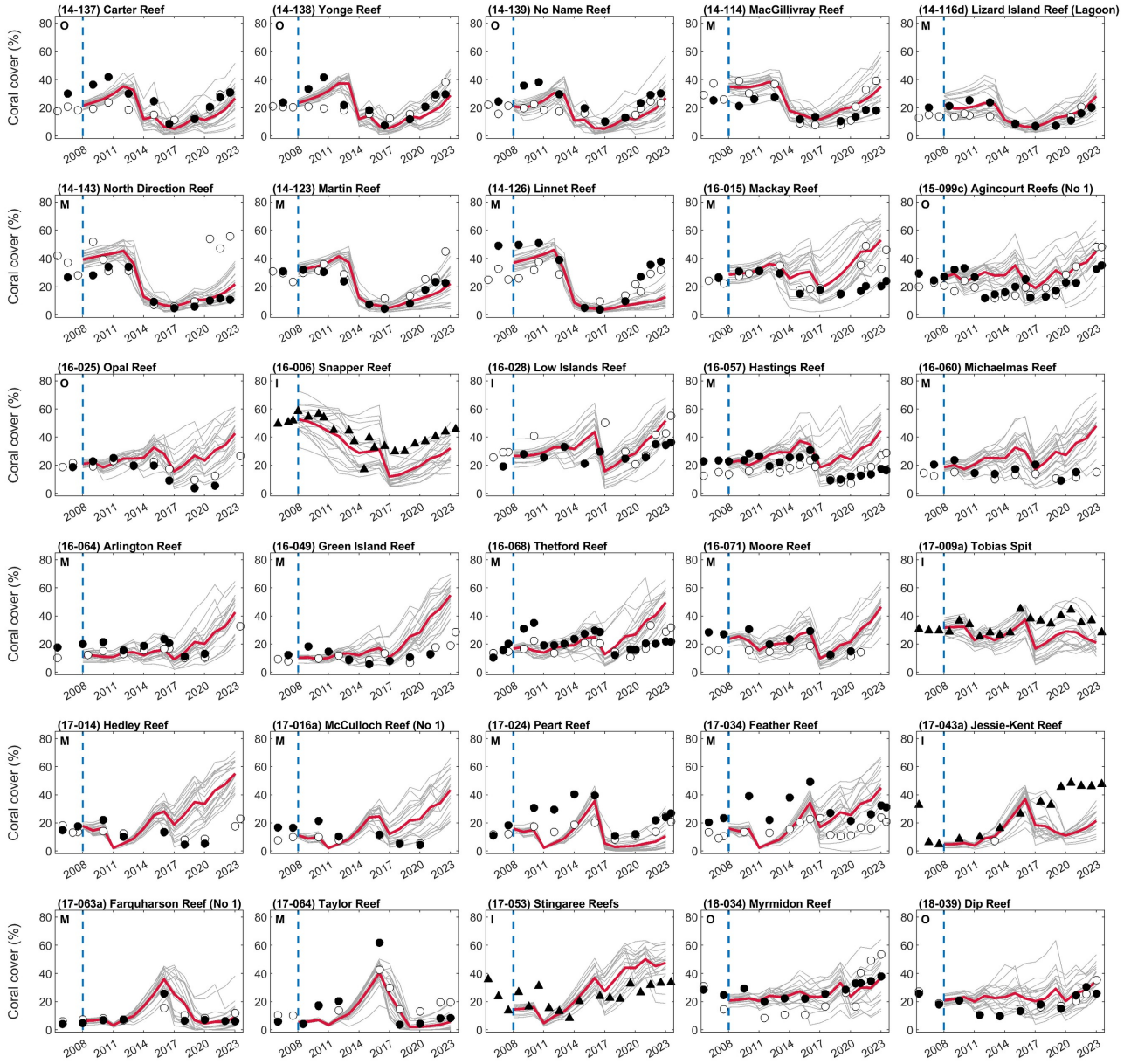

Supplementary Fig. 7. Hindcast (2008–2023) reconstruction of coral cover trajectories at individual reef level. Plots show the simulated (grey lines: stochastic simulations, n = 20; red line: mean trajectory) and observed total coral cover at reefs targeted by the Long-Term Monitoring Program (LTMP) and Marine Monitoring Program (MMP) of the Australian Institute of Marine Science[13] (black dots: LTMP fixed photo-transects; open dots: LTMP manta tows, corrected to transect-equivalent coral cover, see ref. 1; black triangles: MMP fixed photo transects at 5 m depth). The selected reefs have at least one survey between 2006–2008 (used to initialise coral cover in 2008; blue dashed line) and at least nine surveys afterwards. Reefs are ordered from top to bottom following their latitude (as indicated by the two-digit number in their code label), with the northernmost reefs at the top and the southernmost reefs at the bottom. I: inshore; M: mid-shelf; O: outer-shelf.

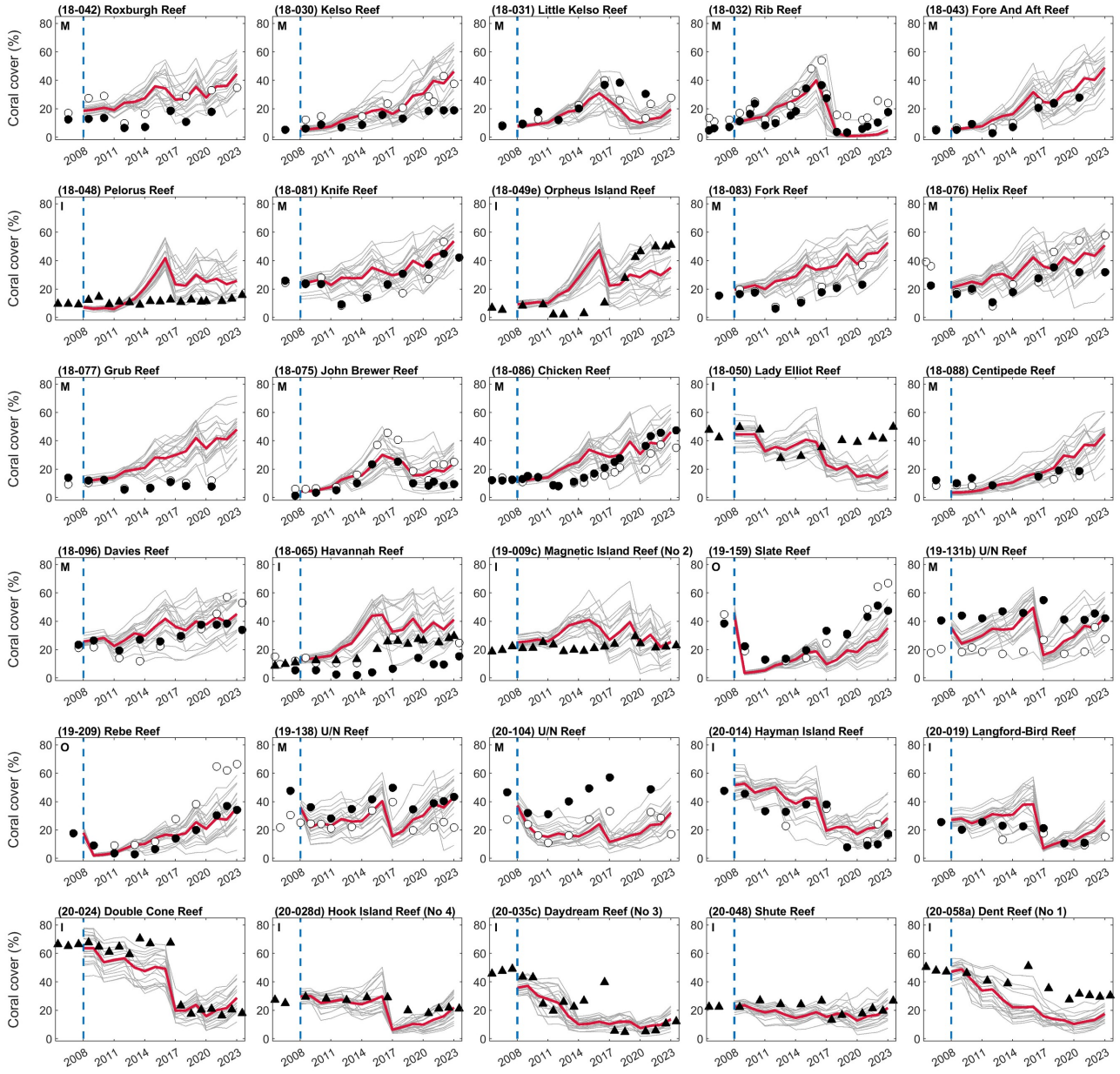

Supplementary Fig. 7 (continued).

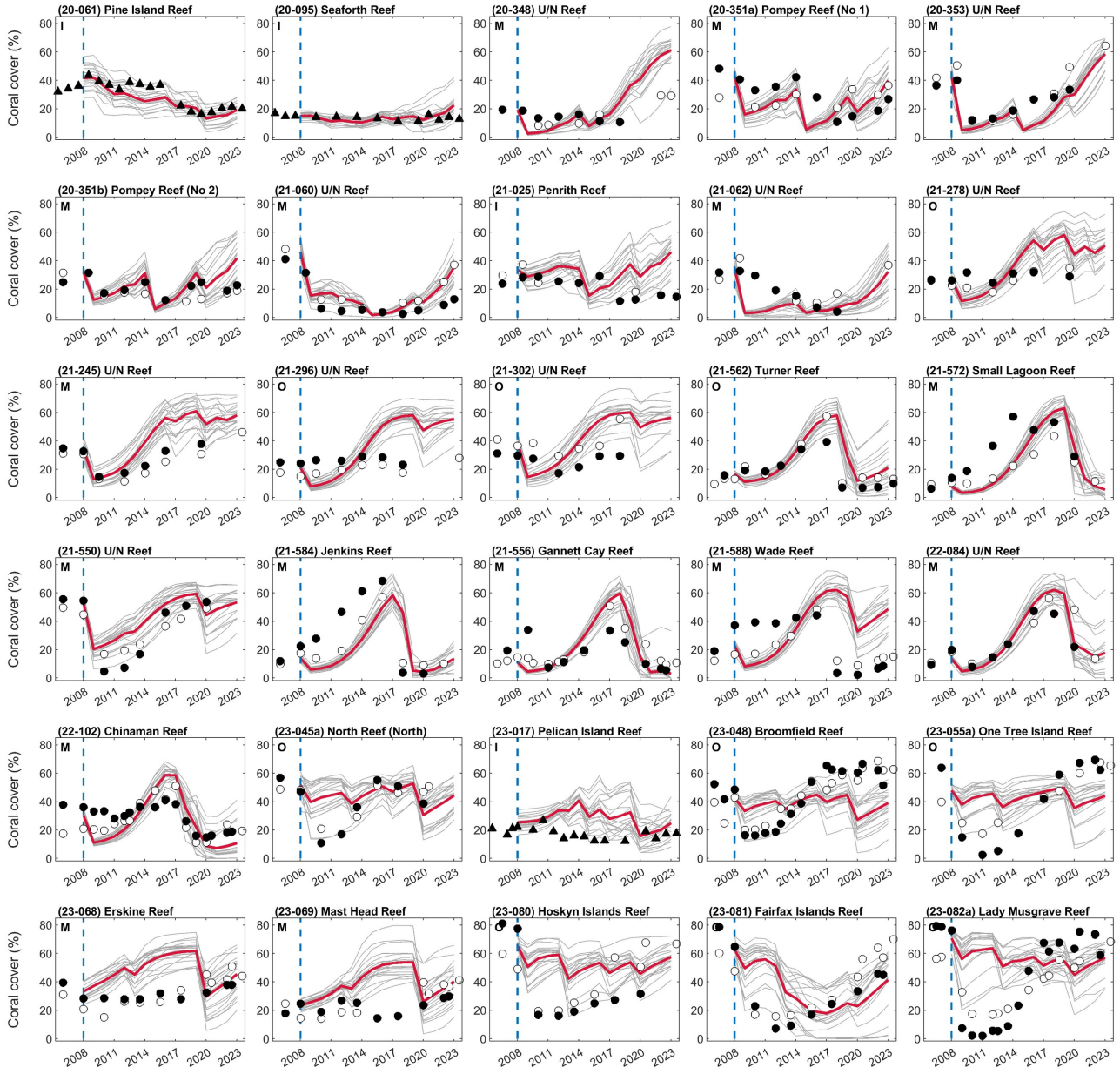

Supplementary Fig. 7 (end).

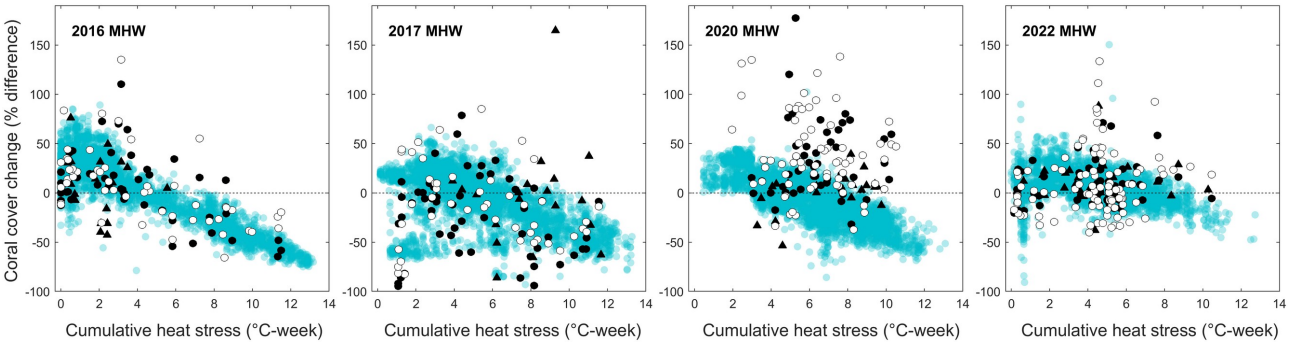

Supplementary Fig. 8. Simulated and observed changes in coral cover after marine heatwaves. From left to right, reef-level relative changes in total coral cover following marine heatwaves (MHW) that occurred across the GBR in 2016 (same as Fig. 1d), 2017, 2020 and 2022, versus their exposure to cumulative heat stress (DHW) derived from satellite observations (NOAA Coral Reef Watch[9]). Simulated coral cover changes (blue dots, n = 3,806 reefs) were captured over a one-year interval. Observed coral cover changes were calculated from monitoring data provided by the Australian Institute of Marine Science[13] Long-Term Monitoring Program (LTMP) and Marine Monitoring Program (MMP): filled black dots, LTMP fixed photo transects; open dots: LTMP manta tow surveys, further converted to transect-equivalent coral cover (see ref. 1); filled black triangles: MMP fixed photo transects (5 m depth). The selected reefs are those monitored within one year before the MHW and again within one year after (2016 MHW: n = 117 reefs; 2017 MHW: n = 119 reefs; 2020 MHW: n = 138 reefs; 2022 MHW: n = 192 reefs). Positive coral cover changes likely indicate the absence of disturbance during the sampled/simulated period, resulting in colony growth and recruitment outweighing natural mortality. Negative coral cover changes underscore the impact of any disturbance, not just marine heatwaves (i.e., tropical cyclones and CoTS outbreaks). Note that bleaching was not simulated when reefs were exposed to 0–3 °C-week heat stress, following ref. 11.

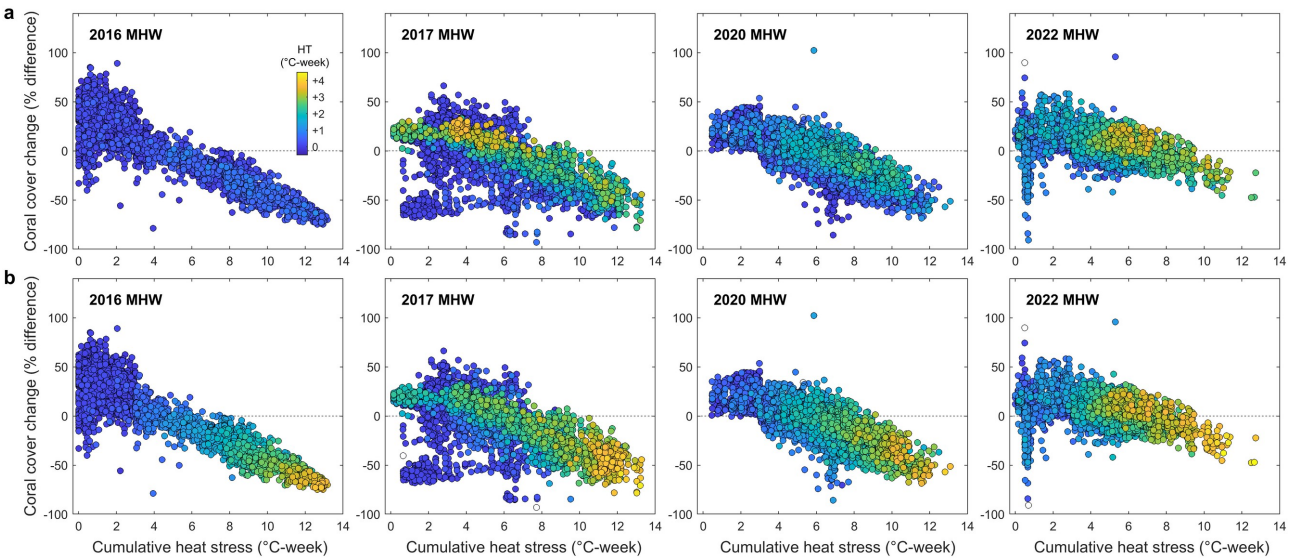

Supplementary Fig. 9. Simulated impacts of recent marine heatwaves on coral heat tolerance. From left to right, relative changes in total coral cover following the 2016, 2017, 2020 and 2022 marine heatwaves (MHW) across the 3,806 simulated reefs as in Supplementary Fig. 8, here showing the mean heat tolerance (HT) of the most sensitive coral groups (acroporids and pocilloporids) before (**a**) and after (**b**) exposure to heat stress. Empty dots denote simulated reefs that did not contain sexually-mature colonies for the selected coral groups, which prevents calculation of mean thermal tolerance.

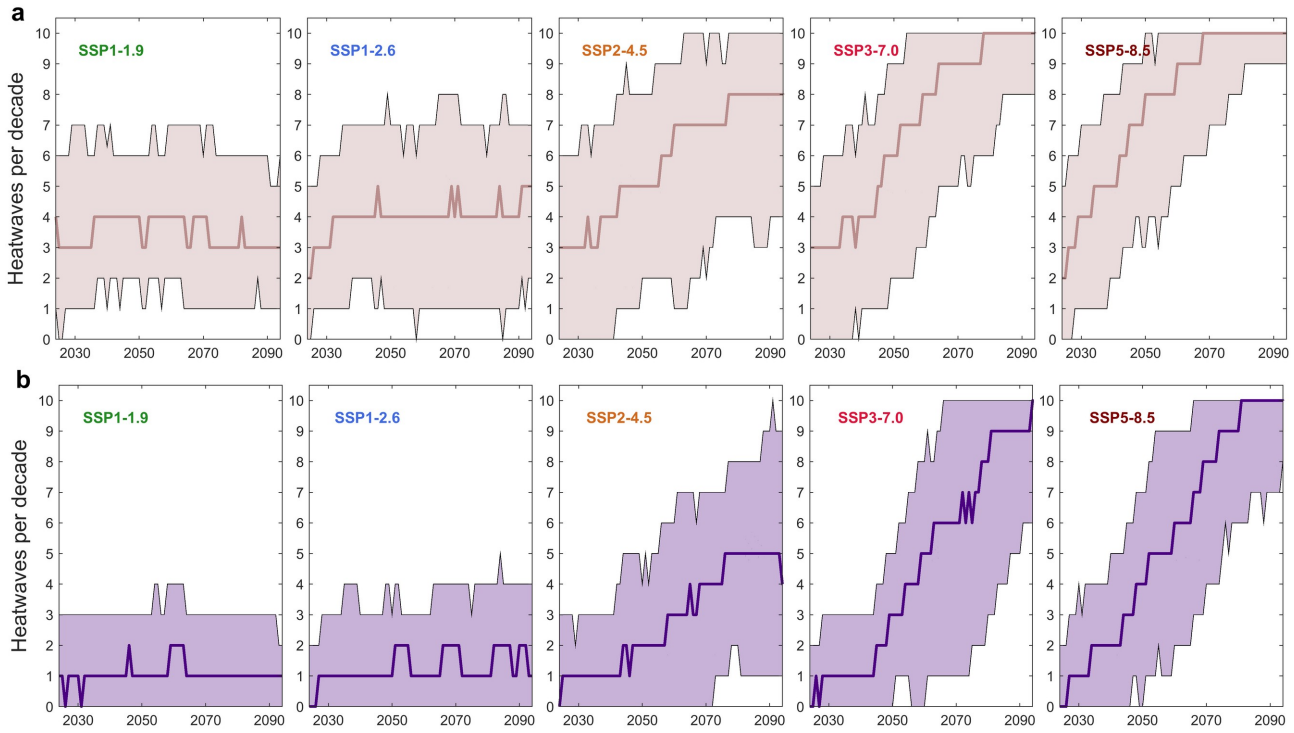

Supplementary Fig. 10. Projected frequency of future severe coral bleaching events. Reef-level decadal frequency of heat stress of severe intensity (**a** DHW > 8 °C-week; **b** DHW > 16 °C-week) experienced across the Great Barrier Reef. For each reef and each year, the number of heat stress events exceeding the specified DHW threshold was calculated using a 10-year sliding window. The bold lines represent the median number of heat stress events across each annual distribution of reef-level values (n = 3,806 reefs × 200 warming futures for each SSP, except for SSP1-1.9). The lower and upper boundaries of the envelop represent the 10th and 90th percentiles, respectively.

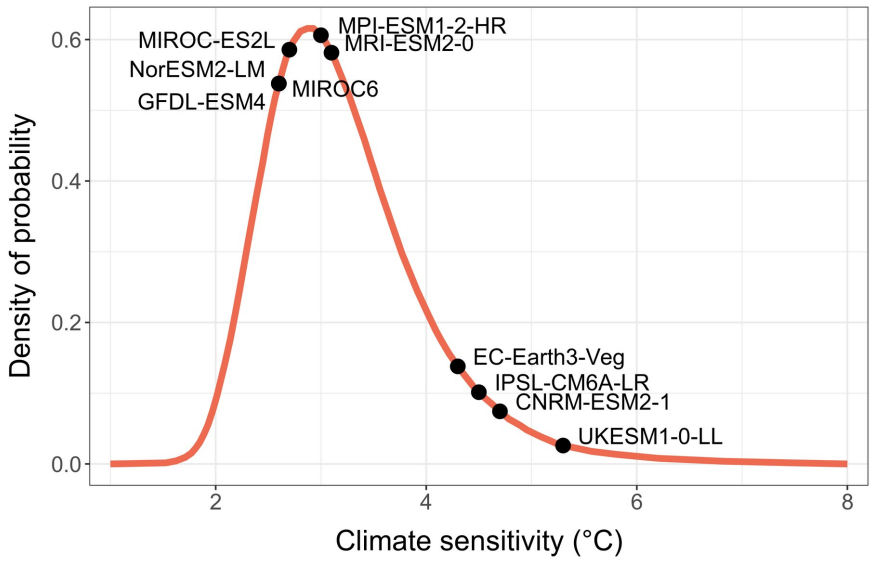

Supplementary Fig. 11. Sensitivity to warming of the ten CMIP6 coupled atmosphere-ocean general circulation models (AOGCMs). AOGCMs are positioned at their respective equilibrium climate sensitivity[15,16] and associated likelihood (red line) based on ref. 14, which conducted a comprehensive evaluation of Earth's climate sensitivity supported by a variety of data and methods. Climate sensitivity refers to the change in global temperature associated to a doubling of atmospheric CO_2 concentrations.

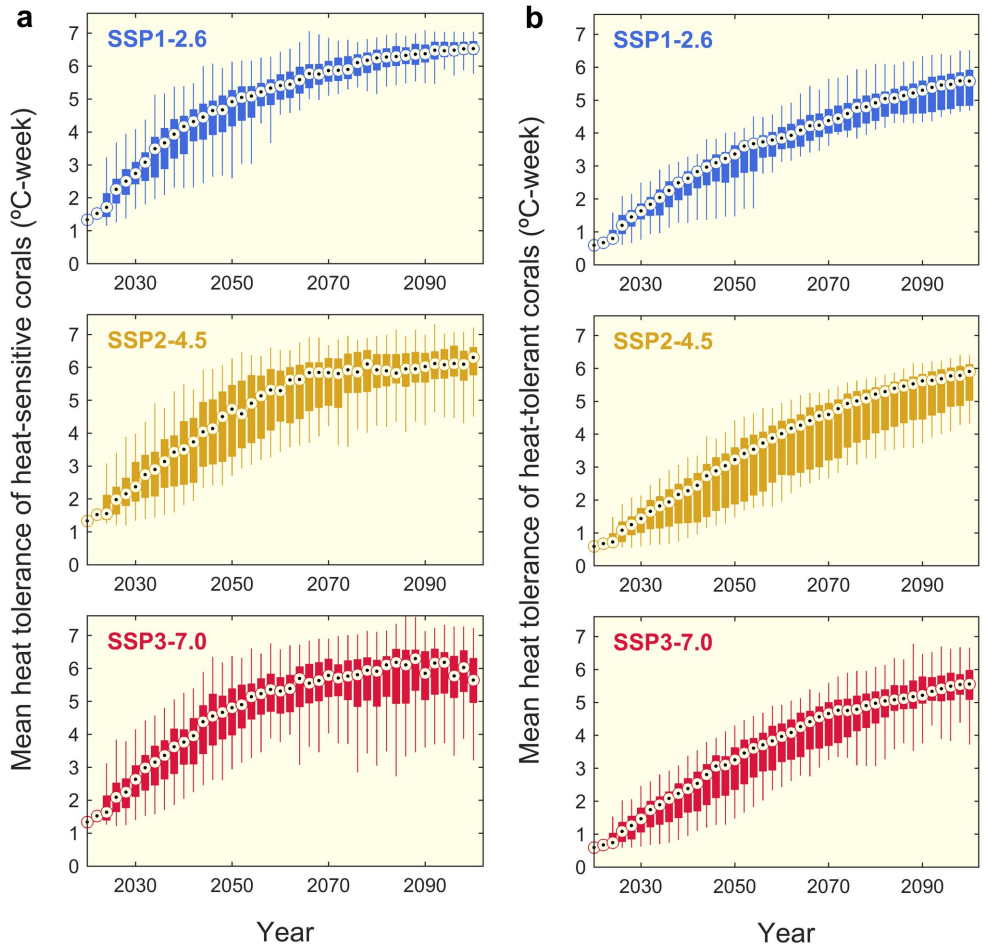

Supplementary Fig. 12. Projections of the GBR mean heat tolerance of corals for the most likely warming futures. From top to bottom, predictions are shown under emission scenarios SSP1-2.6, SSP2-4.5, SSP3-7.0 for (**a**) heat sensitive and (**b**) heat tolerant corals. Heat tolerance is defined as the relative accumulated heat stress (± ºC-week) a coral colony can withstand compared to the mean response of its taxonomic group defined at initialisation. See Fig. 2 legend for the description of box-and-whisker plots (n = 20,000 predictions for each biennial distribution).

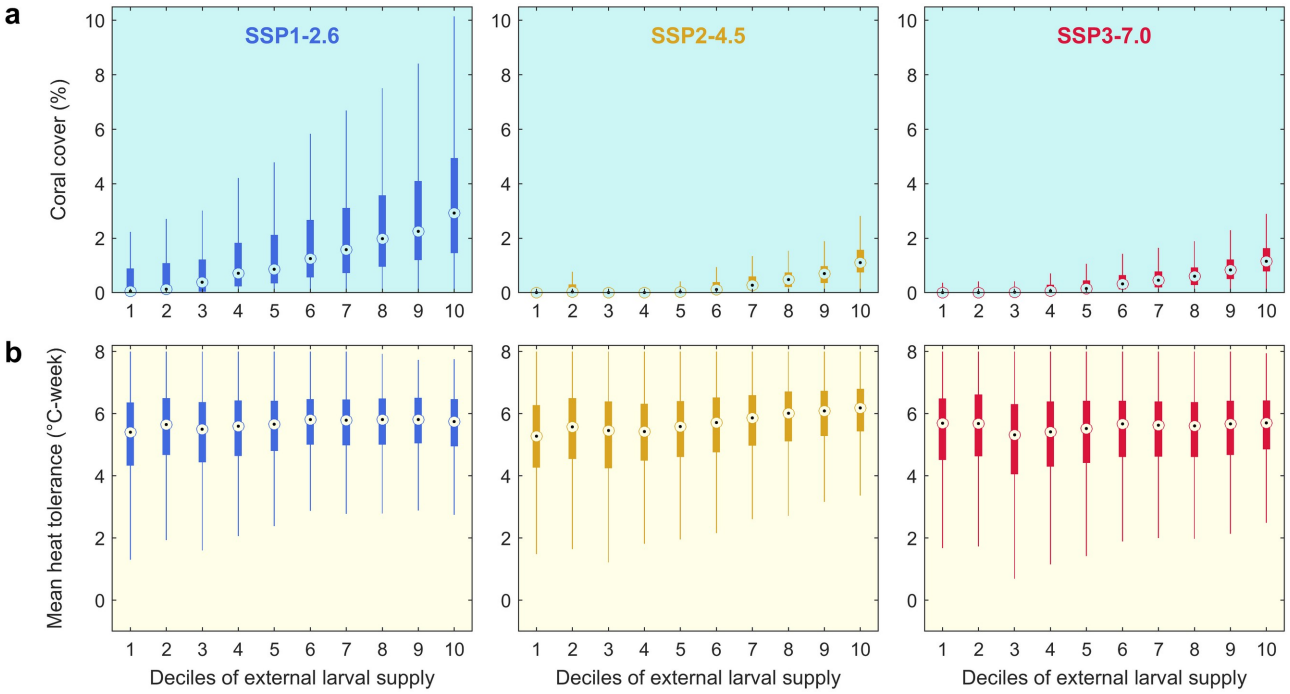

Supplementary Fig. 13. Mid-century projections of coral cover and heat tolerance in warm spots exposed to increased external larval supply. Box and whiskers depict the distribution of (**a**) total percent cover and (**b**) mean heat tolerance of thermally-sensitive coral groups (all acroporids + pocilloporids) predicted in 2050 across warm spots grouped by increasing deciles of external larval supply (i.e., larvae supplied by upstream reefs). External larval supply (larva.m^{-2}) on each reef was averaged over the last five years. As in Fig. 5–6, warm spots are defined as reefs in the top decile of mean DHW calculated over the preceding five years. Inshore reefs (subject to reduced water quality) and reefs affected by cyclones during this period were excluded to maintain focus on heat stress exposure. Resulting distributions across 200 climate projections: n = 20,257 reefs in warm spots in 2050. Boxes and whiskers defined as in Fig. 2 legend.

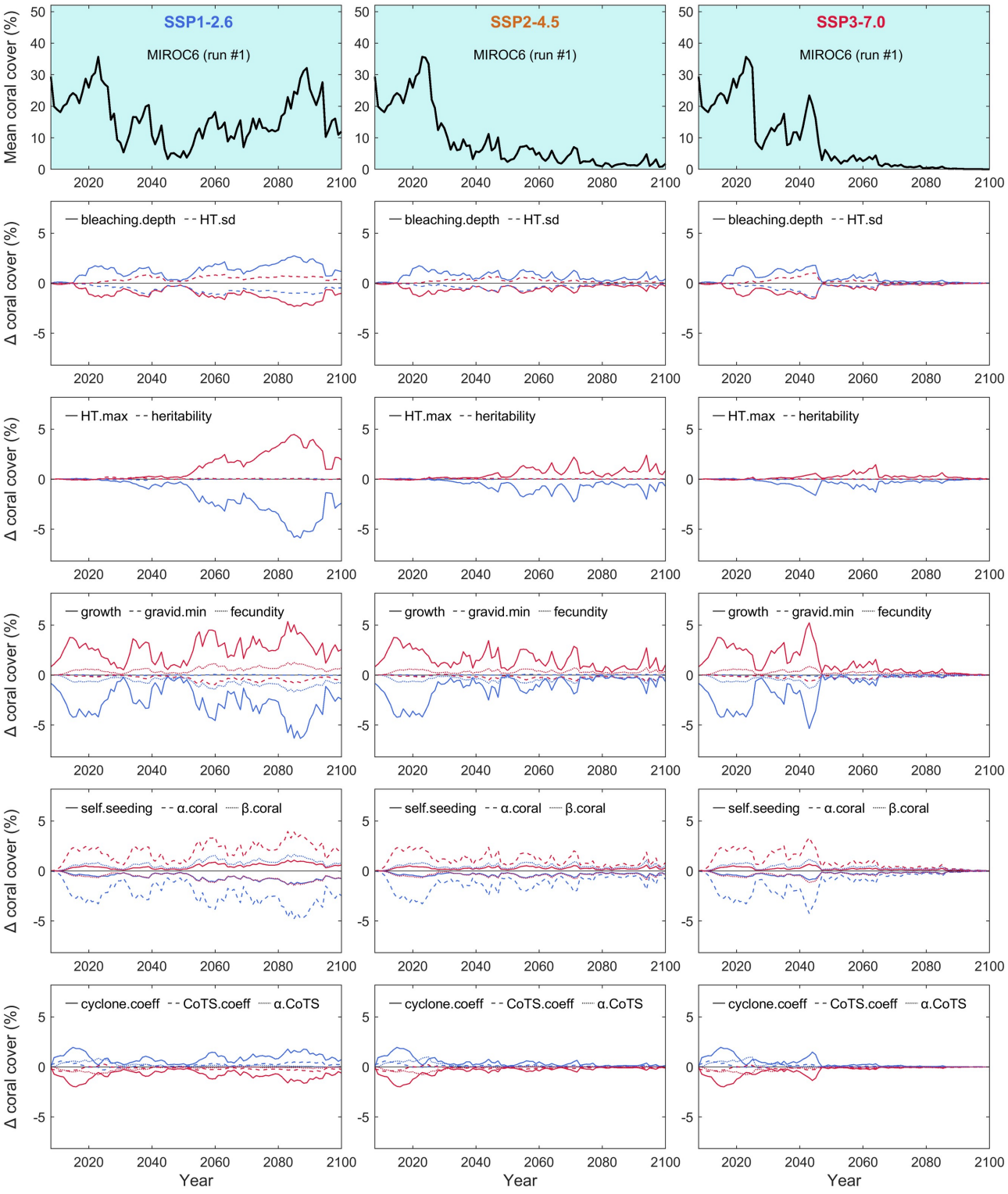

Supplementary Fig. 14. Single-parameter sensitivity analysis on absolute coral cover change. Model sensitivity to key input parameters (Supplementary Table 3) was measured as the difference in GBR mean coral cover (CC, in %) between a simulation where one parameter is varied by ± 20% from its default value (blue: $CC_{-20\%}$; red: $CC_{+20\%}$) and the baseline simulation (CC_{base}, top row) with all parameters at their default values. The difference $CC_{\pm 20\%} - CC_{base}$ was plotted over time for one scenario of future cyclones (run #1) across three SSPs (from left to right) projected by the climate model MIROC-6 (Supplementary Table 1). Parameters α and β define the shape of the larval stock-recruitment relationship for coral and CoTS[1].

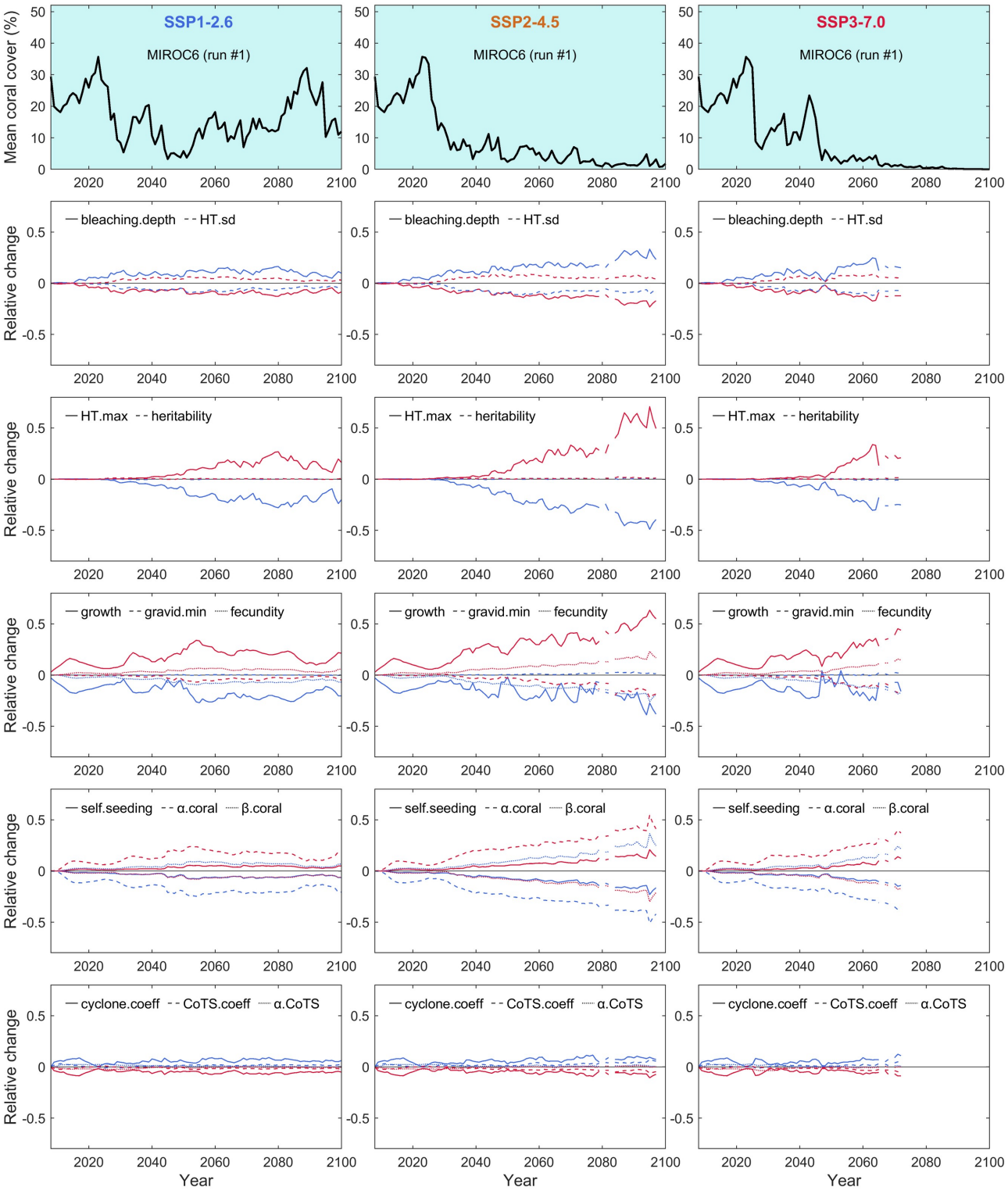

Supplementary Fig. 15. Single-parameter sensitivity analysis on relative coral cover change. Model sensitivity to key input parameters as in Supplementary Fig. 14, here measured as relative change in the GBR mean coral cover compared to the baseline simulation. Relative change was calculated as $(CC_{\pm 20\%} - CC_{base})/CC_{base}$, where a single parameter is varied by ±20% from its default value (blue: −20%; red: +20%), while all other parameters remain at their default values. Relative change was not calculated when the baseline GBR mean coral cover (CC_{base}) was below 1%, as such values can yield disproportionately large relative differences that are not informative at very low coral cover levels.

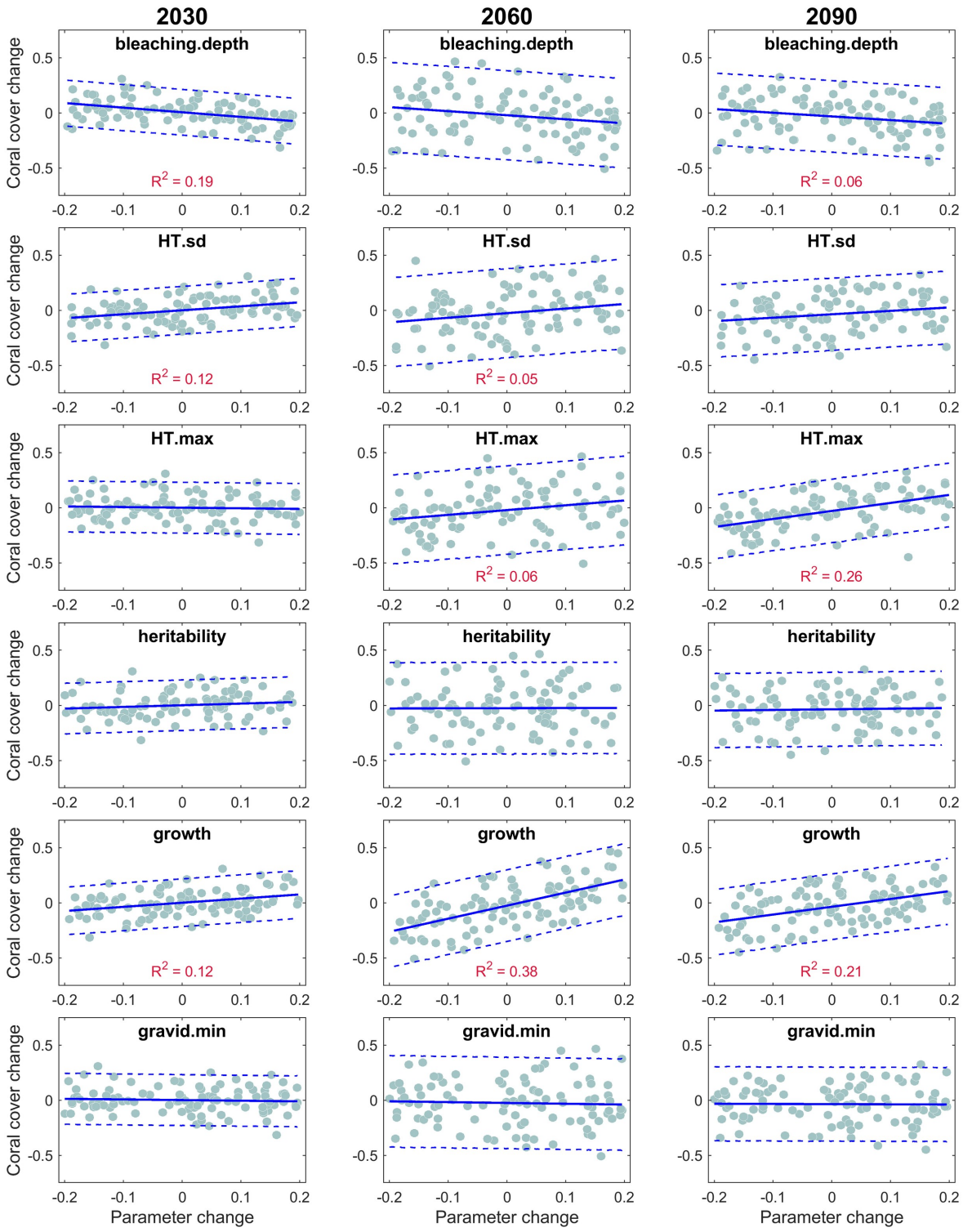

Supplementary Fig. 16. Global sensitivity analysis. Relative change in the GBR mean coral cover obtained after random perturbations of each parameter within −20% and +20% of its default value. Here, 100 simulations of one scenario of cyclones and future warming were run (run #1 of SSP1-2.6 projected by the MIROC-6 climate model – see Supplementary Fig. 14–15) with all parameters sampled at random from a uniform distribution. Relative change was calculated for each simulation i (blue dots) at different time points t (left to right: 2030, 2060, 2090) as $(CC_{i,t} - CC_{base,t})/CC_{base,t}$. Blue lines and dashed lines indicate, respectively, the linear fit and 95% prediction interval. The associated R^2 is indicated in red when above 0.05.

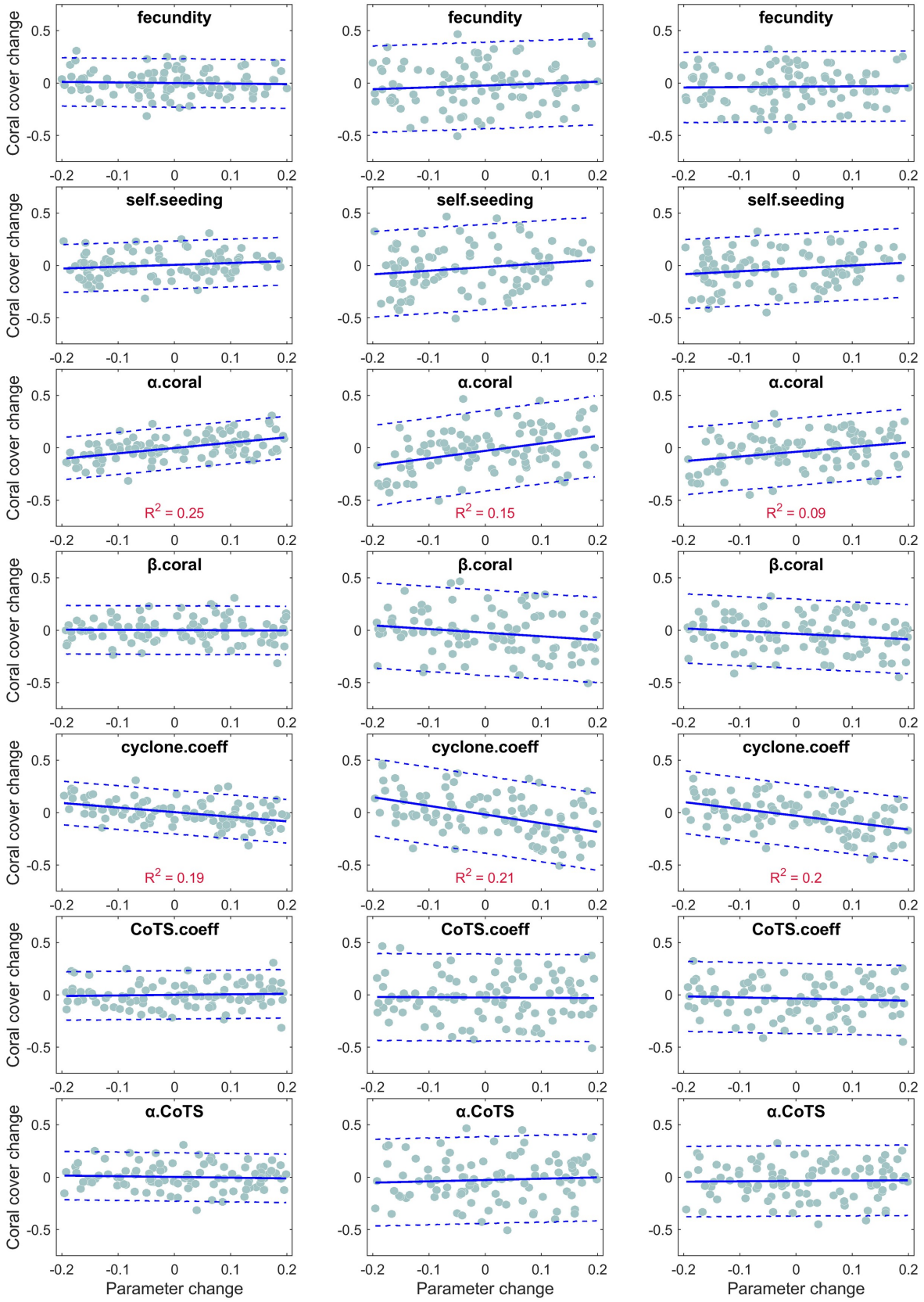

Supplementary Fig. 16 (end).

Supplementary Table 1. Characteristics of the CMIP6 atmosphere-ocean general climate models (AOGCMs) downscaled at 10 km resolution across Australia's Great Barrier Reef. Climate projections (daily sea-surface temperatures) were extracted for five scenarios of greenhouse gas emissions (SSP1-1.9, SSP1-2.6, SSP2-4.5, SSP3-7.0, SSP5-8.5) except for three AOGCMs (indicated with an asterisk) for which SSP1-1.9 was not available. Native spatial resolution after ref. 17. ECS: equilibrium climate sensitivity, after ref. 15.

AOGCM	Reference	Surface resolution (°)	ECS (°C)
CNRM-ESM2-1	18	1.4 × 1.4	4.7
EC-Earth3-Veg	19	0.7 × 0.7	4.3
IPSL-CM6A-LR	20	1.3 × 2.5	4.5
MRI-ESM2-0	21	1.1 × 1.1	3.1
UKESM1-0-LL	22	1.3 × 1.9	5.3
GFDL-ESM4 *	23	1.0 × 1.3	2.6
MIROC-ES2L	24	4.5 × 4.5	2.7
MPI-ESM1-2-HR *	25	~ 0.9	3.0
MIROC6	26	1.4 × 1.4	2.6
NorESM2-LM *	27	1.9 × 2.5	2.6

Supplementary Table 2. Predictors of reef state in mid and late century. State is defined as total coral cover across six diverse coral types. All metrics referenced to either the year 2050 (mid-century) or 2100 (late century).

Predictor (as shown in figure)	Description	Unit	Time frame (years)
Years since bleaching	Number of years since last bleaching event	Years	Variable before each census date
Number of bleaching events	Total number of bleaching events	Events	2025–2050 or 2075–2100
DHW	Mean thermal stress where stress occurs when DHW≥6	°C-week	2025–2050 or 2075–2100
Number of cyclone events	Total number of cyclone events	Events	2025–2050 or 2075–2100
Larval sink strength	Cumulative probability of larvae arriving at reef from other sources	0–1	Annual probability
Years since cyclone	Number of years since last cyclone event	Years	Variable before each census date
Cyclone strength	Mean category of all cyclones affecting the reef during census period	Cyclone category	2025–2050 or 2075–2100
CoTS density	Mean density of adult crown-of-thorns starfish per reef patch	Count per 400 m^2	2025–2050 or 2075–2100
Number of CoTS control events	Number of control events in sampling period	Events	2025–2050 or 2075–2100
WQ impact on recruitment	Proportional coral recruitment after water quality effects where 0 is no recruitment and 1 recruitment unaffected	0–1	Fixed property of reef based on eReefs analysis (see ref. 1)
Years since CoTS control	Number of years since last CoTS control	Years	Variable before each census date
WQ impact on reproduction	Proportional coral reproduction after water quality effects where 0 is no reproduction and 1 implies no impacts on reproduction	0–1	WQ impact on reproduction (see ref. 1)
Larval supply in last 5 years	Cumulative larval supply in 5 years prior to census date, transformed by natural logarithm (+0.1)	Count	2045–2050 or 2095–2100

Supplementary Table 3. List of parameters tested in the sensitivity analysis. Each parameter was varied by ± 20% of its default value (low/high figure), while keeping all other parameters at their default values.

Parameter	Description	Default value	Low figure	High figure
bleaching.depth (w)	Depth-related attenuation coefficient of heat stress	0.43 (7-m depth)	0.34 (~10-m depth)	0.52 (~5-m depth)
HT.sd (σ)	Standard deviation of heat tolerance within each coral group (naive distribution)	2.5 °C-week	2 °C-week	3 °C-week
HT.max	Limits (negative and positive) to heat tolerance within each group	8 °C-week	6.4 °C-week	9.6 °C-week
heritability (h^2)	Heritability (narrow-sense) of heat tolerance	0.3	0.24	0.36
growth	Rate of lateral extension	0.8 – 4.4 cm.yr^{-1}	0.6 – 3.5 cm.yr^{-1}	1.0 – 5.3 cm.yr^{-1}
gravid.min	Size above which a colony is gravid[28] (taxon specific)	31 – 134 cm^2	25 – 107 cm^2	37 – 161 cm^2
fecundity	Parameter *b* of the relationship linking colony size to total egg volume[28] (taxon specific)	1.05 – 2.27	0.84 – 1.82	1.26 – 2.73
self.seeding	Minimum proportion of coral larvae produced on a reef that is retained for recruitment[1]	0.28	0.22	0.34
α.coral	Maximum achievable density of coral settlers for a 100% free space[1] (across all taxa)	15 settler.m^{-2}	12 settler.m^{-2}	18 settler.m^{-2}
β.coral	Density of coral larvae required to produce half the maximum settlement[1] (across all taxa).	75,000 larva.m^{-2}	60,000 larva.m^{-2}	90,000 larva.m^{-2}
cyclone.coeff	Global multiplier of cyclone sensitivity coefficients (obtained after calibration[1])	5	4	6
CoTS.coeff	Global multiplier of CoTS individual consumption rate (obtained after calibration[1])	1.8	1.4	2.2
α.CoTS	Maximum achievable density of CoTS settlers (obtained after calibration[1])	100 settler.m^{-2}	80 settler.m^{-2}	120 settler.m^{-2}

Supplementary Note 1 – Model assumptions and limitations, and their implications

ReefMod-GBR was designed to capture the core dynamics of the Great Barrier Reef (GBR) coral ecosystem, by focusing on the ecological pillars of coral-population fitness (survivorship, growth and reproduction), and how key environmental variables (heat-stress, cyclones, flow-driven larval dispersal, water quality) and ecological factors (coral-eating starfish outbreaks) affect these pillars[1]. Hindcast predictions have been tested against long-term field data[1], providing confidence that the model describes fundamental system dynamics. However, like any model of complex systems, its performance is constrained by the available knowledge and the data that can be gathered across space and time.

We provide below a list of current assumptions and additional processes that might be incorporated in future iterations. Importantly, most of these missing aspects are likely to make our current forecasts more optimistic than reality.

Coral demographics

- Rates of coral growth and fecundity were assumed constant. However, these rates may decline with chronic warming and the intensification of heat stress events. Incorporating the response to warming of these vital rates will likely result in more severe coral declines.
- The model makes an optimistic assumption that fertilisation success is not density dependent, yet critical thresholds in coral density may exist below which coral reproduction becomes ineffective[29]. At very low coral cover levels, adult colonies are likely sparsely distributed leading to insufficient concentrations of eggs and sperm released in the water column. Including such Allee effects on coral reproduction would likely result in worse projections, especially in scenarios with low coral cover.
- The model does not include the demographic impacts of ocean acidification. Physiological studies have shown that high CO2 levels negatively impact coral growth, recruitment and ability to withstand wave damage (see reviews in refs. 30,31). Whether these impacts manifest as changes in coral linear extension or skeletal density is likely to be species specific and known for a handful of species only. However, including the negative impacts of ocean acidification would likely result in lower coral resilience and reef condition, particularly in the latter part of the century. Moreover, ocean acidification may have more important effects on the abundance of calcifying algae that have the potential to impact coral recruitment[32].

Coral heat tolerance

Heat tolerance (HT) of coral individuals is defined relative to the mean bleaching susceptibility of the group at initialisation, with HT=0 ºC-week conferring the bleaching mortality representative of the group. In all coral groups, HT phenotypes are created at initialisation by sampling from a normal distribution of mean 0 ºC-week and standard deviation 2.5 ºC-week following empirical

observations obtained on a single acroporid population (*Acropora digitifera*) from a shallow outer reef crest of Palau[12]. In the absence of similar data on other coral populations, we assumed this distribution to be representative of the present-day (i.e., at the start of simulation in 2008) variability of heat tolerance within each coral group. As the simulation progresses, changes to the HT distributions emerge under the combined effect of bleaching mortality and reproduction, but are constrained within bounding limits (HT_{max}). HT bounding limits of −6 / +6 °C-week would give a representative range of the observed variability of heat tolerance in *Acropora digitifera* (corresponding to the 1st and 99th percentiles of the observed distribution). We extended this range to −8 / +8 °C-week to account for some likely additional variability between species within the coral groups. This may be conservative, with potential to underestimate adaptation, but expanding the bounds further would risk overestimating the scope for adaptation through natural selection.

Given the lack of empirical data for other species, it is currently impossible to directly characterise the variability of heat tolerance within a group. Therefore, we rely on comparisons with *in situ* observations for testing our predicted responses to bleaching. Surveys in the Southern GBR[33] have reported 95% mortality for *Acropora* after the 2024 mass bleaching at 2 m depth under 14.6 °C-week heat stress. Similarly, at Scott Reef (Western Australia), 85% *Acropora* mortality was reported at 9 m depth in response to 13.3 °C-week after the 1998 heatwave[34]. Under similar conditions of depth and heat stress exposure, our model would predict, respectively, 98% and 87% mortality across the three acroporid groups, if not previously exposed to bleaching. This alignment suggests that our model provides a reliable representation of the present-day variability of heat tolerance within these groups.

Natural adaptation to thermal stress

Our coral adaptation model focuses exclusively on phenotypes rather than incorporating genetic or environmental factors that influence coral heat tolerance. To simulate phenotypic adaptation through selection, we employed the univariate breeder's equation which has traditionally been used to predict the evolutionary response of a phenotypic trait from one generation to the next. However, this equation has inherent limitations when applied to our model:

- The breeder's equation was originally designed to estimate changes in a single phenotypic trait under selection within a single generation[35,36]. It calculates the change in the trait based on the selection differential and heritability. We generalised its use for simulating overlapping generations under multiple selective events. Setting the pre-selection distribution of heat tolerance to $t-1$ in the selection differential breaches the breeder's equation assumption that it reflects a true 'pre-selection' state, since it has already been influenced by previous selection events at $t-2$, $t-3$, and earlier. This misalignment with the assumption likely leads to an overestimation of the adaptive potential. The other option is to set the pre-selection value fixed at the initial mean tolerance, but this would lead to an underestimation of the adaptive potential, because it would assume that the trait distribution has not changed over time, ignoring the effects of past selection pressures.
- The breeder's equation primarily addresses genetic adaptation by focusing on heritable traits that are subject to selection. It does not account for phenotypic plasticity, which is the ability of an organism to alter its traits in response to environmental changes within its lifetime[37]. By allowing organisms to adjust their traits without genetic changes, plasticity can either reduce immediate selective pressure on genetic traits, potentially slowing evolution, or

provide temporary adaptive advantages that, under favorable conditions, may lead to genetic changes and accelerate evolutionary adaptation[37,38].

- The model does not account for other critical traits (e.g., colony growth, fecundity) that could be affected by the selection of thermal resistance, yet the enhancement of heat tolerance may come with trade-offs, such as reduced growth[39,40], potentially altering demographic performance. Additionally, rising temperatures may directly affect the performance of those traits. Ignoring negative correlations among multiple traits under selection is likely to overestimate the rate of adaptation[37,41]. On the other hand, positive correlations may result in maladaptations if extensive periods of cool temperatures occur between heatwaves.
- We assumed that heritability does not change throughout 21st century. While this may be a reasonable assumption considering the short timescale (~100 years) of the simulated evolution (few generations), heritability is not a fixed attribute and can change even after few decades[42]. While the magnitude of these changes are unknown for the inheritance of coral heat tolerance, integrating temporal variations would likely affect our projections, towards a greater scope for coral adaptation if heritability increases, and an opposed effect if heritability decreases, resulting in more severe coral declines.
- The potential for coral adaptation to warming also depends on the level of thermal tolerance achieved by the symbiotic algae[43]. Rates of thermal adaptation in symbiont populations and the capacity of the coral host to shift to more heat tolerant symbionts (i.e., symbiont shuffling) might both interact with its capacity of adaptation[44]. However, the outcome of this interaction is difficult to anticipate.

Environmental drivers

- Given that the downscaled temperature projections for the period 2014–2023 tend to predict more severe heat stress than observed in satellite data (see Supplementary Fig. 4b), the frequency and intensity of future marine heatwaves may be overestimated, at least in the early years of the forecast. As a result, the predicted coral decline over the next 1–2 decades may be overestimated, and the potential for coral adaptation underestimated.
- If raw climate projections exhibit a temporal periodicity of heat stress within particular decades, this would be altered by the random shuffling of DHW years that was applied at subdecadal scale for creating 20 stochastic warming futures for each climate projection. If such periodicity exists, and assuming it is accurately represented in climate projections, marine heatwaves will tend to occur in clusters, with recovery period slightly extended compared to our stochastic projections, although this would not only be perceptible in the most mitigated warming scenarios (SSP1-1.9, SSP1-2.6) as heat stress under higher emissions (SSP2-4.5, SSP3-7.0, SSP5-8.5) occur at high frequency, right from the early years of projections.
- While our selection include four climate models with relatively low equilibrium climate sensitivity (ECS = 2.6 – 2.7 °C, Supplementary Table 1, Supplementary Fig. 11), only few climate models from the larger available ensemble exhibit lower values (3 models in a compilation of 34 climate models from ref. 15,16). Including such models in the very low-end of ECS could provide more optimistic scenarios of future warming in our weighted ensemble.

- While we implicitly assumed that larval dispersal will remain unchanged in the future, ocean circulation could be modified by climate change[45]. Moreover, characteristics of larval development could be affected, with warmer temperatures increasing larval mortality and/or reducing larval competency[46]. Any of these changes would affect the contemporary routes of larval dispersal and connectivity.
- Spatio-temporal patterns of suspended sediment[1] were also assumed to remain unchanged in the future.

Supplementary Methods 1 – Estimation of the 3D surface area and carrying capacity of individual reefs

Individual reefs included in ReefMod-GBR are defined following earlier coral connectivity studies[3] that represented the Great Barrier Reef (GBR) network with 3,806 reefs based on a Geographic Information System map ("*Great Barrier Reef Features*") of indicative reef outline[47]. A first version of the model[1] used the 2D planar area of each reef polygon delimited by this indicative outline as an estimate of the corresponding reef area. During simulations, individual reef areas are scaled up from a representative 400 m^2 grid lattice (20×20 cells of 1 m^2 of reef substratum) to true reef areas when calculating the total amount of offspring produced before dispersal. Recent mapping of reef geomorphic zonation (0 – 20 m depth range) and benthic categories (0 – 10 m) have produced estimates of the 3D surface area of reef substrate using high-resolution (10×10 m pixels) satellite-derived reflectance data and bathymetry[48]. These two mapping products offer a unique opportunity to refine individual reef areas for more accurate estimates of coral population sizes and reproductive potential.

We converted the GBR *geomorphic* raster pixels[48,49] into polygons using ArcGIS Pro. This operation only included four geomorphic categories dominated by hard substrate and considered as suitable habitat for corals[48]: Outer Reef Flat, Reef Crest, Sheltered Reef Slope, and Reef Slope. Geomorphic polygons were then overlaid onto the *Great Barrier Reef Features* shapefile, thus creating a link between the geomorphic polygons and the identifier (UNIQUE_ID) of the indicative *reef* polygons. The 2D areas (in km^2) of *geomorphic* polygons of a given class that fell within a *reef* polygon were combined and summed to produce an estimate of the 2D area of coral habitat for each individual reef. As a result, 1,086 reef polygons of the original indicative reef outline remained unassociated to a 2D estimate of coral habitat area due to discrepancies between mapping products. Because these reefs are currently integrated into the management plans established by the Great Barrier Reef Marine Park Authority (GBRMPA), we extrapolated the area of coral habitat based on linear regression models between indicative reef area (as predictor) and 2D geomorphic area of coral habitat (as response) where both estimates were available. Regression models were built separately for inshore, mid-shelf and outer-shelf reefs. Since geomorphic categories were also available as slope-adjusted 3D surface areas (derived from a locally-estimated bathymetric gradient, see details in ref. 48), the 2D area of coral habitat on every single reef was converted into 3D surface area based on a linear regression model established from the available reef-level 2D/3D area estimates (Supplementary Fig. 17). As a result, the total 3D area of coral habitat across the 3,806 reefs amounts to 13,842 km^2, with individual reef areas ranging from 5 m^2 to 133.53 km^2 (median: 0.67 km^2).

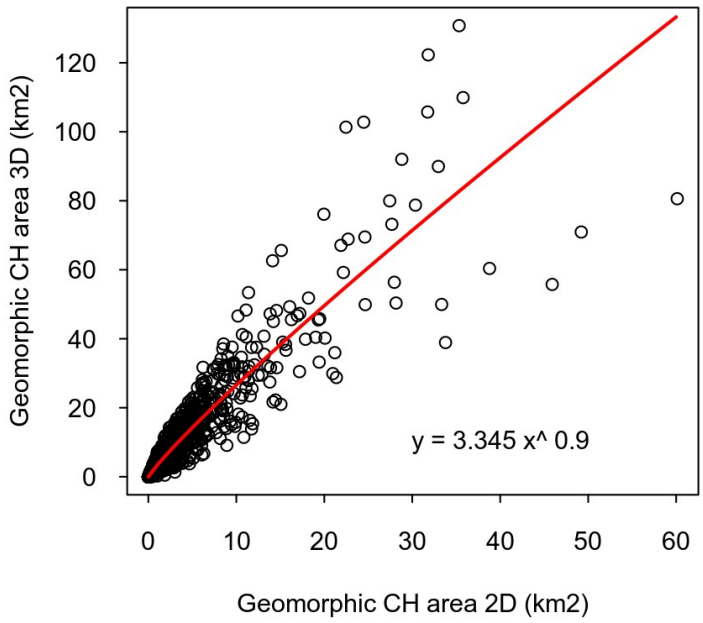

Supplementary Fig. 17. Relationship between 2D and 3D estimates of coral habitat area produced by satellite-based reef mapping across the GBR. Coral habitat area of individual reefs (n = 3,033) corresponds to the summed area of four geomorphic categories: Outer Reef flat, Reef Crest, Sheltered Reef Slope and Reef Slope.

For any given reef, ReefMod accounts for a proportion of the reef area that is effectively colonised by corals given the amount of hard, consolidated substratum present on a reef. This excludes patches of sand and sessile organisms that are not explicitly modelled, such as sponges and soft corals, and essentially sets a maximum value to coral total percentage cover (hereafter referred to as coral cover carrying capacity). We first estimated the proportion of sand in every reef using the GBR *benthic* mapping product[48]. The shapefile of geomorphic polygons was overlaid over the *benthic* raster pixels[28] across four benthic cover classes: Sand, Rock, Rubble, and indiscriminate Coral/Algae. Since the benthic and geomorphic maps do not encompass the same depth range (0 – 10 m vs. 0 – 20 m, respectively), this overlay created pixels with an undefined benthic cover type (i.e., 'NA') for geomorphic polygons in the 10 – 20 m depth range. Undefined benthic areas were filled with Sand, Rock, Rubble, and Coral/Algae under the assumption they each extend to the 20 m isobath proportionally to their relative contribution to the 0 – 10 m geomorphic layer. Finally, regression models between the area of coral habitat (predictor) and the area of each of the four benthic cover categories (response) were developed to extrapolate benthic cover areas to the reef polygons with missing geomorphic/benthic cover data. The four benthic categories were expressed as proportion of the 2D area of coral habitat within each individual reef.

Considering that a suitable space for coral colonisation includes coral/algae (substratum currently colonised), rock (substratum available to colonisation) and rubble (substratum available to colonisation once consolidated) but not sand (unconsolidated substratum), our first objective was to accurately estimate the cover of sand on every reef based on the satellite-derived benthic map pixels. Although each 10×10 m pixel is assigned a specific type of benthic cover[48], this does not imply that each pixel consists entirely of the assigned benthic type. Instead, this assignment indicates the predominant cover within a given pixel (having largest proportional cover), yet other benthic types could be present. We conducted simulations to generate 1,000,000 virtual benthic configurations, randomly allocating proportional cover for each of the four benthic types. We

assumed that, within a configuration, the proportional cover of each type is independent of one another and that the overall sum equals 1. For each benthic type we isolated the configurations where it is predominant and found that its mean cover approaches 0.42 over the selected configurations. We thus assumed that 42% is the representative (i.e., average) proportional space of the predominant benthic type assigned to a 10×10 m pixel, while the remaining space (58%) is shared among the other three benthic covers (given that none of them exceeds 42%). Therefore, we estimated for every reef the mean proportional cover of sand ($SAND_{reef}$) across all benthic types as:

$$SAND_{reef} = 0.42 \cdot Sand_{reef} + 0.58/3 \cdot (Coral/Algae_{reef} + Rock_{reef} + Rubble_{reef})$$

Because Sand, Coral/Algae, Rock and Rubble sum to 1 on every reef, this comes down to:

$$SAND_{reef} = 0.23 \cdot Sand_{reef} + 0.19$$

Reef-specific values of proportional sand cover were combined with regional cover of sponges and soft corals derived from monitoring observations. The average proportional cover of soft corals (SC_{shelf}) and sponges (SP_{shelf}) was calculated from monitoring data across the continental shelf of the GBR[13] (Supplementary Table 4).

Supplementary Table 4. Average proportional cover of sponges and soft corals across the GBR. Cover estimates were calculated from the photo-transect survey database (1992–2017) of the Australian Institute of Marine Science (AIMS) Long-Term Monitoring Program (LTMP)[13].

Benthic category	Inshore reefs	Mid-shelf reefs	Outer-shelf reefs
Soft corals	0.10	0.08	0.14
Sponges	0.01	0.01	0.02

Coral cover carrying capacity (K_{reef}) was then estimated on every individual reef as:

$$K_{reef} = 1 - SAND_{reef} - SC_{shelf} - SP_{shelf}$$

As a result, coral cover carrying capacity across the 3,806 reefs ranges from 49.1% to 71.9%, with an average value of 66.5%, 69.6% and 63.9% for inshore, mid-shelf and outer-shelf reefs, respectively (Supplementary Fig. 18).

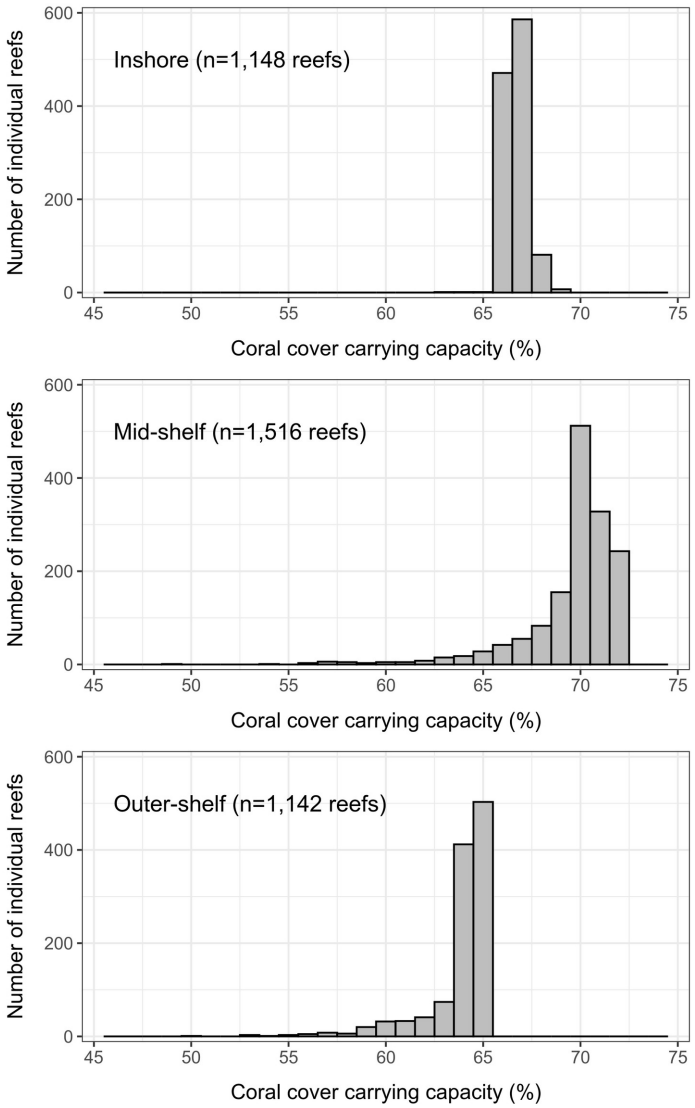

Supplementary Fig. 18. Reef-level coral carrying capacity across the GBR. Reef distribution of coral carrying capacity as the maximum percentage of reef area that can be colonised by corals for inshore, mid-shelf and outer-shelf reefs.

Supplementary Methods 2 – Fine-scale coral community modelling (C~scape)

The C~scape modelling framework[50] combines coral demography with information on the major processes that vary spatially within reefs and influence coral population growth and mortality, to simulate coral metacommunity dynamics (Supplementary Fig. 19).

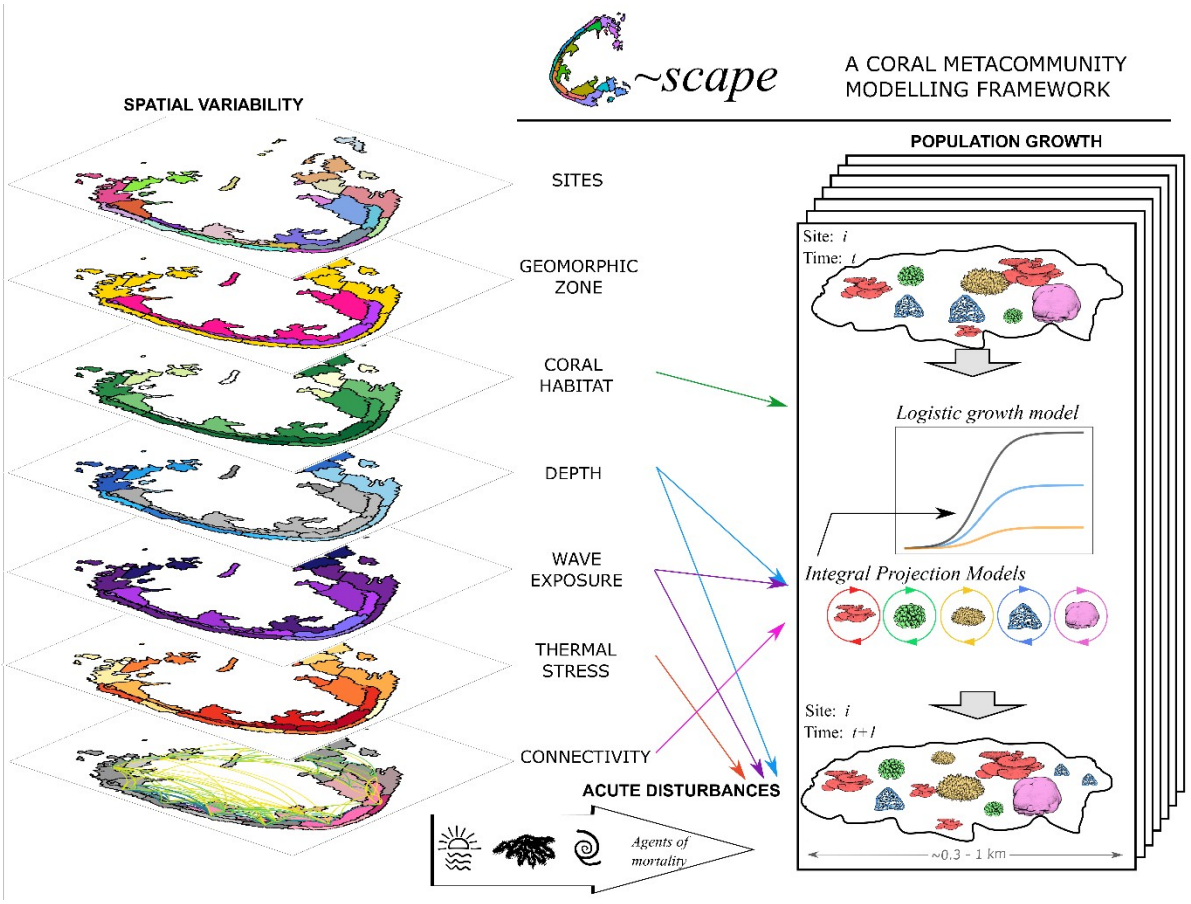

Supplementary Fig. 19. Schematic representation of the C~scape modelling framework. The C~scape model[50] is applied to a reef or cluster of reefs. A reef is divided into multiple spatial units referred to as 'sites'. A 'population' for each distinct coral type is modelled discretely at each site. Metapopulations are connected with a connectivity matrix describing the probability of coral larvae moving among sites. Intrinsic population growth rates are determined for each coral type from integral projection models (IPMs) that describe the coral life cycle, enabling the projection of changes in each population of corals over an annual period from time t to time t+1. The IPMs contain discrete life states for coral eggs, larvae and settlers, as well as a continuous state across the size range of each coral type captured by 100 size classes. Sites have different depths, influencing the populations' exposure to temperature stress. Sites are assigned a value for the 'coral habitat', which specifies the maximum percentage total coral cover in a site; this value modulates community growth as the maximum is approached. Acute disturbances (temperature stress, cyclones and crown-of-thorns starfish outbreaks) affect coral populations by killing individuals as function of their disturbance intensity. Icons from A. Cresswell.

For the present study, the C~scape model was run for a cluster of five offshore reefs in the Central Great Barrier Reef – the 'Moore Reef cluster' (Supplementary Fig. 20) – with the same environmental forcing as applied in ReefMod-GBR, i.e., using the same 20 stochastic DHW projections paired with future cyclone tracks for a total of 47 climate realisations. We simulated coral cover dynamics for five coral types in C~scape to match as closely as possible with the simulations conducted in ReefMod-GBR.

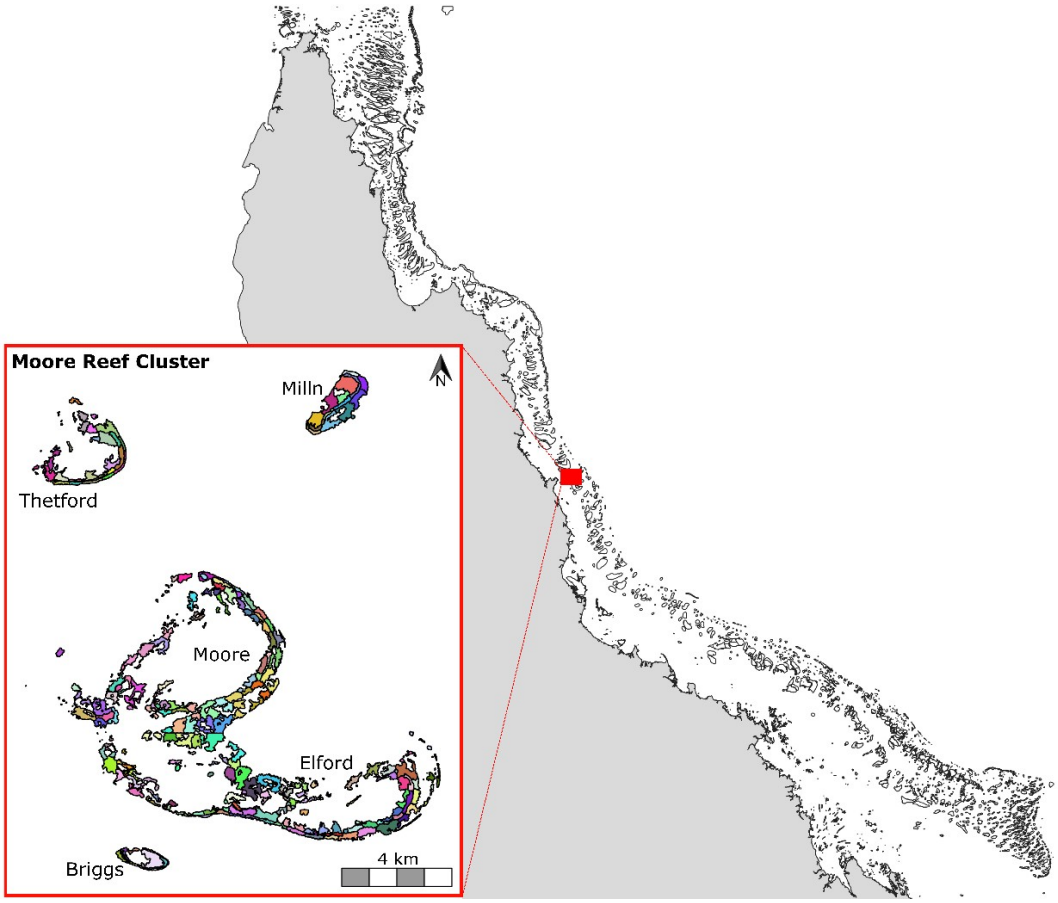

Supplementary Fig. 20. Spatial location of the Moore Reef cluster in the Central Great Barrier Reef. The inset shows the five reefs (Thetford, Milln, Moore, Briggs and Elford) and their division into sites (randomly colorised for enhanced visualisation). Reef and habitat (inset) polygons mapped using the geospatial datasets 'Great Barrier Reef Features (GDA94)' and 'GBR10 GBRMP Geomorphic', both publicly available from the Reef Geohub platform (https://reef-geohub-ext-geohubgbrmpa.hub.arcgis.com/).

The C~scape modelling framework is designed to capture variation in coral demographics within individual reefs, and therefore any one reef is broken into numerous spatial units. The spatial units are delineated as a spatially explicit mosaic of 'site' polygons across the modelled geographic area. Environmental conditions are assumed to be homogeneous within each site.

Coral demographics within each site are modelled using a logistic ordinary differential equation modified such that the intrinsic growth rate is substituted for the growth rate obtained from Integral Projection Models (IPMs, refs. 50–51). The IPMs are based on the coral life cycle, with the major processes of growth and survival informed by Bayesian regressions built from annual samples of many individual coral colonies for each of five distinct coral types. The IPMs allow projections of the annual probability of growth and survival, and the amount of reproductive material produced in a site by a group of coral populations of a defined type (Supplementary Table 5) as a function of

coral colony size and other covariates. To account for changes in coral growth and survival due to local site variables such as limits on available suitable habitat, depth and wave exposure, the IPMs are allowed to vary as a function of these parameters, thus generating site-specific population dynamics. Coral demographics are modelled separately within each site but are connected via the transport of coral larvae to and from other sites, as informed by connectivity matrices, allowing simulation of metacommunity dynamics across the cluster.

The C~scape metacommunity modelling framework is fully detailed in ref. 50 with an application to the Moore Reef Cluster for hindcasting coral dynamics between 2008 to 2022. Here, we have simulated the same location with various model developments to include future projections:

- the expansion of coral functional types to include tabular acroporids, corymbose/digitate acroporids, corymbose non-acroporids, small massive/ sub-massive and large massive coral groups;
- spatially explicit IPMS for generating site-specific population growth;
- An explicit distribution of heat tolerance across coral individuals as opposed to a single mean value per coral type;
- coral adaptation to heat stress driven by selection.

In the following we detail the main differences from the previous modelling approach[50]. We also detail how we downscaled to a site-level from the same environmental forcing as used by the ReefMod-GBR model simulations.

Site delineation and characterisation

The geographic boundaries of reefs were determined from the same publicly available geomorphic zonation map as used by ReefMod-GBR that depict the distribution of geomorphic features such as reef crest, slope, or lagoon[48]. We only considered the zones that are expected to have predominantly hard substrate (Reef Slope, Reef Crest, Outer Reef Flat and Sheltered Reef Slope) to be areas where we would expect appropriate habitat and conditions for corals to grow[48,52]. Each reef zone was taken separately and further partitioned to account for other spatially varying processes (e.g., connectivity, depth). The geomorphic zones were pixelated and a Euclidean distance matrix was created to cluster pixels together using the function ‘hclust’ (method: ‘complete’) of the R Stats package[53]. In this way, hexagons within the same geomorphic zone and adjacent to each other were clustered together to form a ‘site’ polygon that had a maximum longest diameter of ~1,000 m (see ref. 50 for full details on how sites were delineated).

Once sites are delineated, they are characterised by their depth, wave exposure and proportion of suitable coral habitat. The site polygons were overlaid on a bathymetric map of pixel size 10×10 m (https://www.eomap.com/) to determine the mean depth within each polygon. The site polygons were also overlaid on a map of modelled wave exposure[54] (‘ubed mean’ from the SWAN model https://espace.library.uq.edu.au/view/UQ:8246441) to assign the median wave exposure per site. Ubed mean is the mean horizontal velocity at the seafloor, and gives an indication of how much force water movement at the seafloor is exerting on corals, influencing their growth and survival via physical impact and through the transfer of nutrients from the water to the corals.

Each site has a two-dimensional (2D) area according to the boundaries of its polygon. However, some parts of a reef can be very sloping, and therefore may have larger area than captured by the planar area. A three-dimensional (3D) area was calculated for each site using a “surface-to-

horizontal-area ratio" derived from the slope value estimated for each pixel. Slope was estimated by using a local gradient method (3×3 m window) from the bathymetric map. The slope-adjusted surface area, i.e., 3D surface area, was calculated using the trigonometric formula:

$A_{3D} = A_{2D} / \cos(slope)$

where *slope* is expressed in radians.

In the Moore Reef Cluster, a total of 213 sites were delineated (Supplementary Fig. 20), with 3D areas ranging from 1 – 20 ha (median 9 ha). Benthic category maps[48] were used to calculate the actual proportion of 3D surface area that is available for coral colonisation. In this mapping product, each 10×10 m pixel is classified as one of four benthic categories: Sand, Rubble, Rock, Coral/Algae. Site polygons were overlaid on the benthic map and the number of pixels of each of the four categories were used to determine the proportion of suitable habitat for corals by assuming Sand and Rubble were not appropriate substrates[50]. As a result, the proportional area of coral colonisation across the Moore Reef cluster ranged from 20 – 66% (median 59%) per site.

Coral groups and population growth

The C~scape modelling framework has IPMs at its core and these are informed by Bayesian regressions built from annual samples of individual coral colonies[50]. C~scape therefore has growth, survival and fecundity rates that are functions of colony size[50]. This means the demographic rates of growth and survival are different from the parameterisations in ReefMod-GBR, which are structured around different size classes, but comparable in capturing the major differences in growth and survival between functional types. The coral groups simulated for the present study (Supplementary Table 5) are similar to the groups simulated in ReefMod-GBR, with the absence of staghorn acroporids, which form thickets, rather than having clear individuals, and therefore did not align well with an IPM framework.

Supplementary Table 5. Summary description of the five coral types modelled in the C~scape metacommunity model. The description includes parameters that relate to discrete transitions in the IPMs.

Coral group	Tabular acroporids	Corymbose/ digitate acroporids	Corymbose non-acroporids	Small massive/ sub-massive	Large massive	Source
Description	Acroporids with flat, plate-like structures with horizontal growth and fused branches	Dense, bushy acroporids. Corymbose corals have a single stem. Digitate corals have the entire base of the colony attached to the seafloor. Branches are not fused	Dense, bushy, growth forms of non-acroporid corals that reproduce predominately via broadcast spawning – i.e. releasing eggs and larvae into the water column	Mound-like semi-spherical or spherical shaped colonies (not including *Porites*)	Mound-like semi-spherical or spherical shaped colonies of the *Porites* genus, that can grow to very large sizes	
Genera used to parameterise growth and survival	*Acropora*	*Acropora*	*Pocillopora*, *Seriatopora*, *Stylophora*	*Favites*, *Goniastra*, *Platygyra*	*Porites*	Unpub. data*
Genera used to inform fecundity	*Acropora hyacinthus*	*Acropora millepora*	*Stylophora pistillata*	*Goniastrea retiformis*	*Goniastrea retiformis*	[28]
Fertilisation to larvae	55% of spawned eggs assumed to get fertilised in the water column					[29]
Early mortality prior to dispersal	50% of larvae assumed to die prior to becoming competent to settle (e.g. predators, natural mortality)					[55]
Settlement	Probability of settlement parameterised as 2.1% of larvae will settle if over reef substrate within the larvae competency window (see ref. 50)			Settlement probability was assumed to be 60% that of the tabular and corymbose groups.		[56–58]
Growth to 1-year old coral	1.315% probability of transitioning from the discrete ‘settler’ state to the continuous state.					[59]
Size at 1-year old	Sampled from a normal distribution with mean 2.56 cm and standard deviation 0.26 cm.			Sampled from a normal distribution with mean 1.41cm diameter and standard deviation 0.14 cm		[57,58]

* Data collected across the Great Barrier Reef by the Reef Restoration and Adaptation Program, https://gbrrestoration.org/program/ecorrap/

Annual coral population growth in C~scape is modelled using a logistic ordinary differential equation modified such that the intrinsic growth rate is substituted for the growth rate obtained from IPMs for each coral type. The intrinsic population growth rate $r_{\_ft\_i}$ for coral type *ft* and site *i* is based on an integral projection matrix (see supplementary information 2 in ref. 50). Here, growth and survival regressions were expanded to include variables for wave exposure and for depth, based

on the sites where colonies were measured. This meant it was possible to create site-specific IPMs at a function of the depth and wave exposure assigned to each modelled site.

To create the IPMs, coral growth and survival data were provided by the EcoRRAP program that monitors ~40 different sites on the Great Barrier Reef (https://gbrrestoration.org/program/ecorrap/) using photogrammetry and juvenile quadrats to follow colonies over annual periods such that change in size and survival could be statistically modelled as a function of colony size (Supplementary Fig. 21).

Specifically, growth was modelled as:

$$log(colony\ area)\ time\ t+1 \sim log(colony\ area)\ time\ t + depth + wave\ exposure + (1|Site)$$

Survival was modelled as:

$$survival\ t+1 \sim log(colony\ area)\ time\ t + depth + wave\ exposure + (1|Site)$$

Further detail on fitting the Bayesian regressions to build the IPMs is provided in ref. 50 with the main difference here being the inclusion of the additional variables for depth (a fixed categorical factor either shallow (~ 5 – 8 m) or deep (~ 8 – 14 m)) and wave exposure modelled as the horizontal water velocity on the seafloor ('ubed mean')[54].

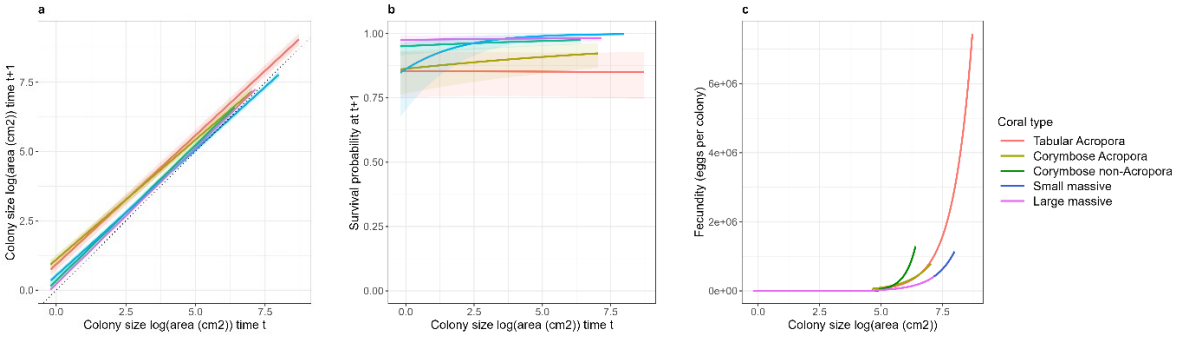

Supplementary Fig. 21. Coral size-based vital rates implemented into the C~scape model. Predictions from Bayesian regressions for the vital rates (**a**) growth, (**b**) survival and (**c**) fecundity that are incorporated into building the IPM transition matrices.

Fecundity was calculated as a function of the simulated abundance and size of colonies within a site at any given time point. The amount of eggs produced was parameterised here using the same functions as in ReefMod-GBR, originally sourced from ref. 28.

To account for changes in coral growth and survival due to limits on available suitable habitat, the IPMs are modulated by a coral habitat parameter that defines the maximum total coral cover in a site. Research in modelling coral populations has shown that different functions within the logistic family may be appropriate to represent population growth in different scenarios[60,61]. Within the logistic family of functions the main difference is the amount of asymmetry between the increase in acceleration of the per capital rate in the early part of the function and the reduction in acceleration as carrying capacity is approached. Here we use the crowding function:

$$D_{i,t} = \frac{K_i - C_{i,t} - C_c}{K_i}$$

where K_i is the carrying capacity at site *i* based on the proportion of suitable habitat, and $C_{i,t}$ is the total coral cover at site *i* at time *t* and C_c is the total coral cover at the location and time of data collection from EcoRRAP.

We apply $D_{i,t}$ during the calculation of the transition probabilities contained within the IPM matrix. This enables us to explicitly target growth rather than growth and survival, as there is not clear empirical evidence to demonstrate a reduction in survival as space is depleted. Once the probabilities of growth independent of density dependence and chronic temperature are calculated using the Bayesian regression models, we apply the density dependence:

$$g(x,y)_{ft,i,t} = D_{i,t} * g(x,y)_{ft,i,D=1}$$

where $g(x,y)_{ft,i,D=1}$ are the growth probabilities based solely on the Bayesian regression models.

Environmental forcing and downscaling

Temperature stress, cyclones, and Acanthaster Crown-of-Thorns starfish (COTS) outbreaks are implemented as acute disturbances in the C~scape framework in a similar way to in ReefMod-GBR. In any given year these disturbances can impact coral population by killing coral colonies within a site. The intensity of these disturbances at the reef level, i.e. for each of the five reefs simulated by C~scape, is the same as for the ReefMod-GBR simulations, such that both models received the same environmental forcing through time.

Cyclones are implemented uniformly across all sites within a reef. Output from ReefMod-GBR simulations for each scenario gave the density of COTS per m^2 for each reef in each year. The reef level density was apportioned between sites within reefs by multiplying by the total site area, such that larger sites received more COTS.

Site-level downscaling was conducted for heat stress. As detailed in ref. 50, variability in heat stress across the reef cluster was modelled in historic marine heatwave years using the eReefs RECOM model[62] at 250 m resolution. We did this for the period from 1 November in the preceding year through to 30 April in the named years for 2016, 2017 and 2020 (i.e., years with the historically higher acute thermal stress). We modelled surface DHW, as depth was handled separately in the coral mortality functions (see section 'acute disturbance mortality'). From this modelling we assigned a DHW value to each site in the cluster for the three modelled heatwave years. We then calculated the mean DHW for each modelled heatwave year and each reef. We then calculated the proportional residuals ($R_{i,y}$) between the DHW of a site and the mean DHW value of all sites within the reef for the three marine heatwave years that were modelled using RECOM:

$$R_{i,y} = \frac{DHW_i - \frac{\sum DHW_i}{n}}{\frac{\sum DHW_i}{n}}$$

where i=1 to n for each of the 213 sites in the Moore Reef cluster and y is each of the marine heatwave years (2016, 2017, 2020).

Next, the mean and standard deviation of the residuals were calculated for each site across the three years (Supplementary Fig. 22) to allow the fitting of a normal distribution. These values were then used as a scaling parameter to downscale the reef level DHW timeseries, which were the common

input to both ReefMod-GBR and C~scape. Calculating a scaling parameter in this way meant that in any year taking the average of all the sites DHW values for a reef would give the reef-level DHW, while creating site-level variability in temperature stress, as determined from the finer-spatial scale RECOM modelling.

Using the scaling parameters, we calculated for each site $DHW_{i,t}$ for each time t and for each climate model and climate scenario for which we had a reef level DHW value, $DHW_{reef,t}$:

$$DHW_{i,t} = DHW_{reef,t} + DHW_{reef,t} \cdot rnorm\left(mean\left(R_t\right), std\left(R_t\right)\right)$$

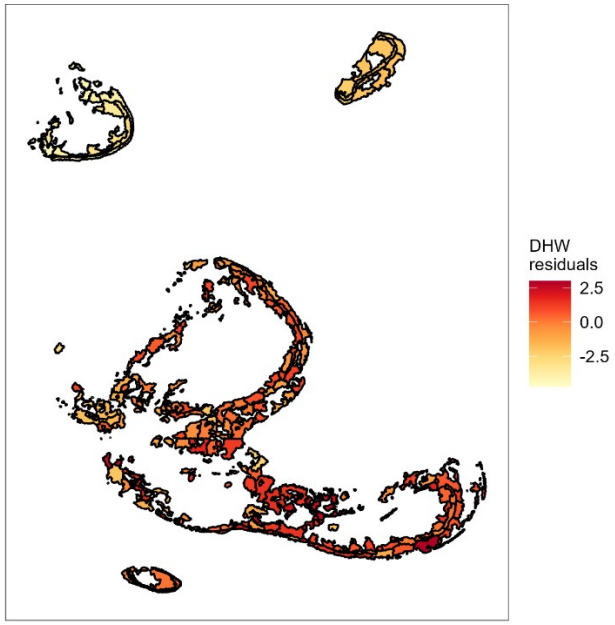

Supplementary Fig. 22. The mean Degree Heating Week residuals across the three marine heatwave years modelled. The residuals are used in multiplication with the reef level DHW predictions to give a site-level DHW.

Acute disturbance mortality

Mortality due to cyclones and COTS are detailed in ref. 50. Cyclone mortality is simpler than that captured by ReefMod-GBR in that it is a function only of windspeed and coral type and does not account for other factors such as coral size and processes such as sand scouring. COTS mortality is applied in the same way as in ReefMod-GBR, where mortality is a function of the abundance of COTS and size-dependent consumption rates.

Heat stress mortality is modelled using the same functions as applied in ReefMod-GBR (see main text) but modified to be site-specific by accounting for the depth of a site:

$$m_{init_{ft}} = w_{site} \cdot s_{ft} \cdot \left(\left(e^{0.17 + 0.35 \cdot DHW_{site}}\right) - 1\right) / 100$$

with w_{site} being the depth coefficient and s_{ft} being the bleaching sensitivity of a species (same sensitives as applied as for ReefMod-GBR parameterisation).

The depth coefficient was calculated as:

$$w_{site} = e^{-0.07551 \left(sitedepth - 2\right)}$$

Annual mortality (M) was then calculated as described in the main text to give (Supplementary Fig. 23):

$$M_{ft_{site}} = 1 - \left(1 - m_{init_{ft_{site}}}\right)^{6}$$

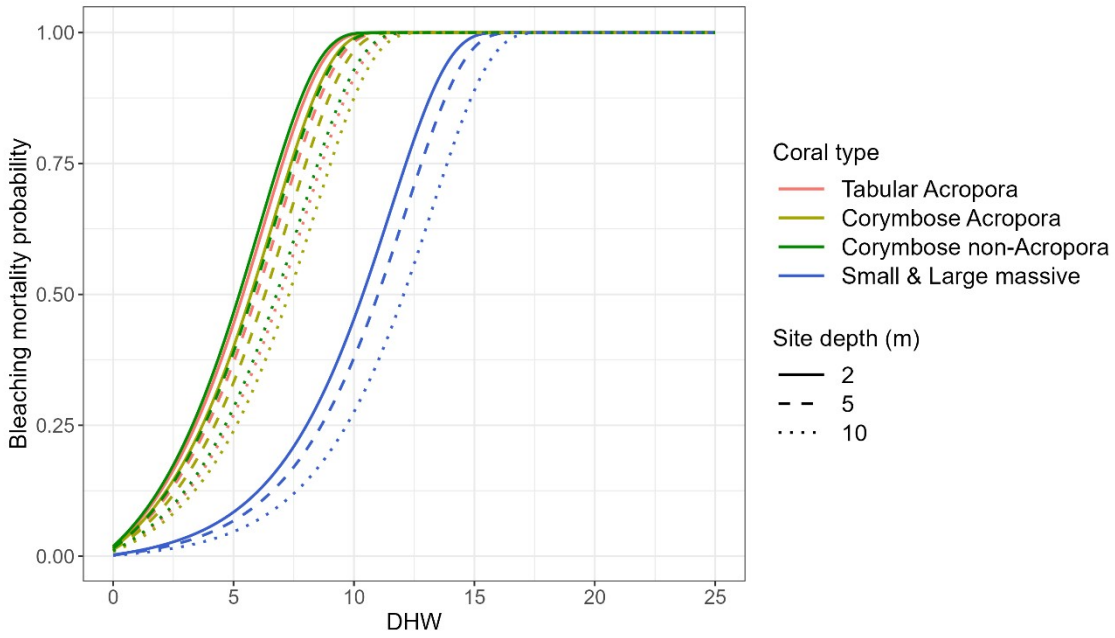

Supplementary Fig. 23. Bleaching mortality probability as a function of the DHW at a site shown for each of the different coral groups at three depths.

Heat tolerance

In C~scape, natural selection and adaptation are modelled based on phenotypic variance rather than attempting to create a gene-based model. This assumption was necessary due to the complexity of genetic models as well as insufficient data availability.

We define heat tolerance of an individual as the deviation from the mean bleaching mortality response of the population. Hence, we can add a heat tolerance term, $^{\Delta DHW}$, to the initial bleaching mortality:

$$m_{init_{ft_{site}}} = w_{site} \cdot s_{ft} \cdot \left(\left(e^{0.17 + 0.35 \cdot \left(DHW_{site} - \Delta DHW\right)}\right) - 1\right) / 100$$

This implementation shifts the bleaching mortality curve for heat stress events along the x-axis (Supplementary Fig. 24) to allow for more heat tolerant individuals ($^{\Delta DHW > 0}$) and less heat tolerant individuals ($^{\Delta DHW < 0}$).

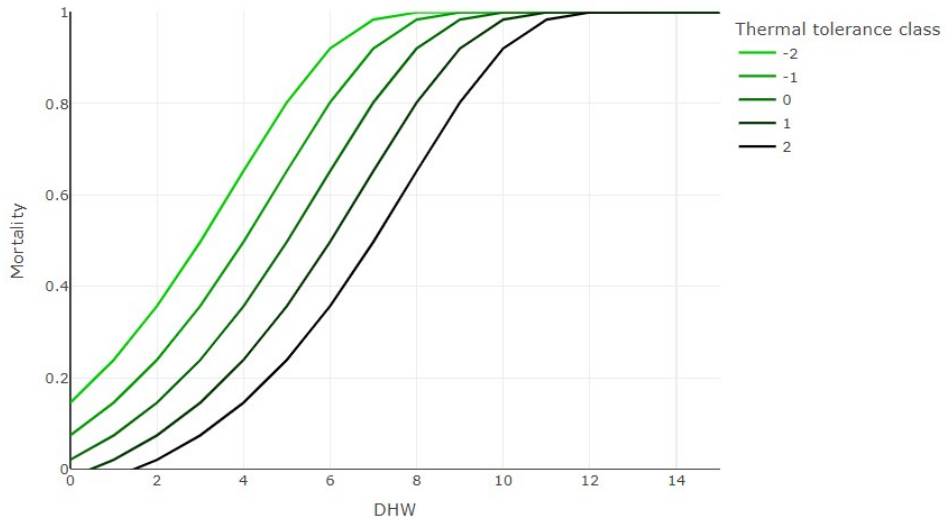

Supplementary Fig. 24. Heat stress mortality curve for tabular acroporids at site depth=0m for heat tolerance, δDHW , classes ranging from −2 to 2DHW.

Implementing these heat tolerances classes meant we modified what had previously been $N_{ft,i,t}$ (ref. 50), a vector of the number of corals of coral type *ft* in each of the 100 size classes and three discrete life stages (eggs, larvae and settlers) at time *t* and site *i* to instead be a two-dimensional matrix describing the number of corals in each size classes-heat tolerance class combination. The number of heat tolerance classes can be assigned based on the research question and the scenarios a user is interested in. Here we used available data from ref. 12 and extrapolated the identified Bleaching Mortality Index (BMI) curves to 100% mortality, since this was the only point where BMI and the mortality curves used in C~scape were comparable (Supplementary Fig. 25). While this is similar to the ReefMod-GBR parameterisation, the calculated distribution differs due to slight differences in the shape of the bleaching mortality curves implemented in ReefMod-GBR versus C~scape and consequently, different extrapolation was necessary. The difference in °C-week between the 10th and 90th percentile calculated at 100% mortality is ~ 4.91 °C-week, which results in a normal distribution with $sd = 1.91$ (Supplementary Fig. 26). As infinite heat tolerance is not realistic, we cut-off the normal distribution at −8 and +8 °C-week heat tolerance ($|HT_{max}|$= 8 ºC-week), which means that the heat tolerance classes encompass > 99.99% of the normal distribution and is aligned with the ReefMod-GBR implementation.

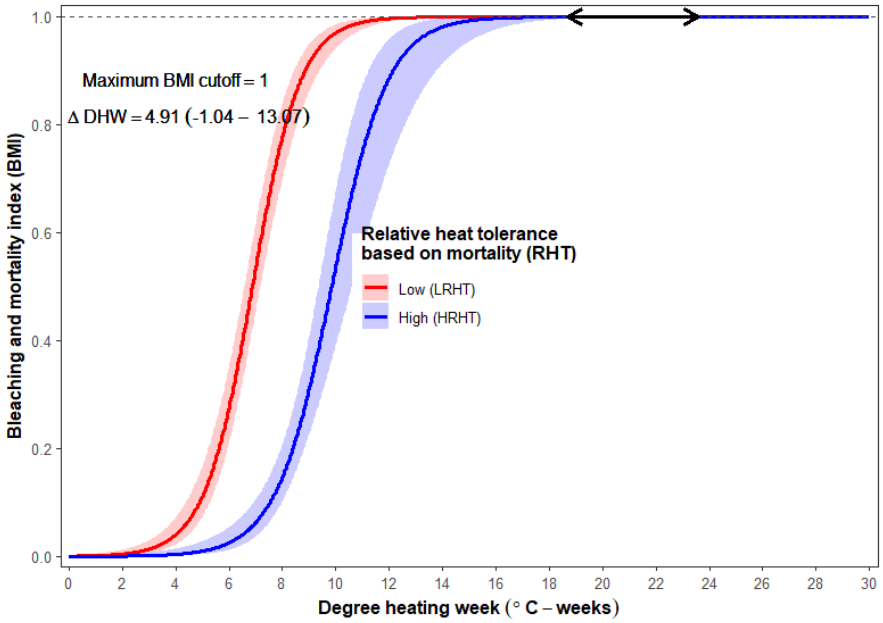

Supplementary Fig. 25. Bleaching Mortality Index as per ref. 12 extrapolated to BMI=1 based on the C~scape implementation of heat tolerance on the bleaching mortality curve. The red line shows the mortality response of the 10% least heat tolerant corals and blue shows the response for the 10% most heat tolerant corals.

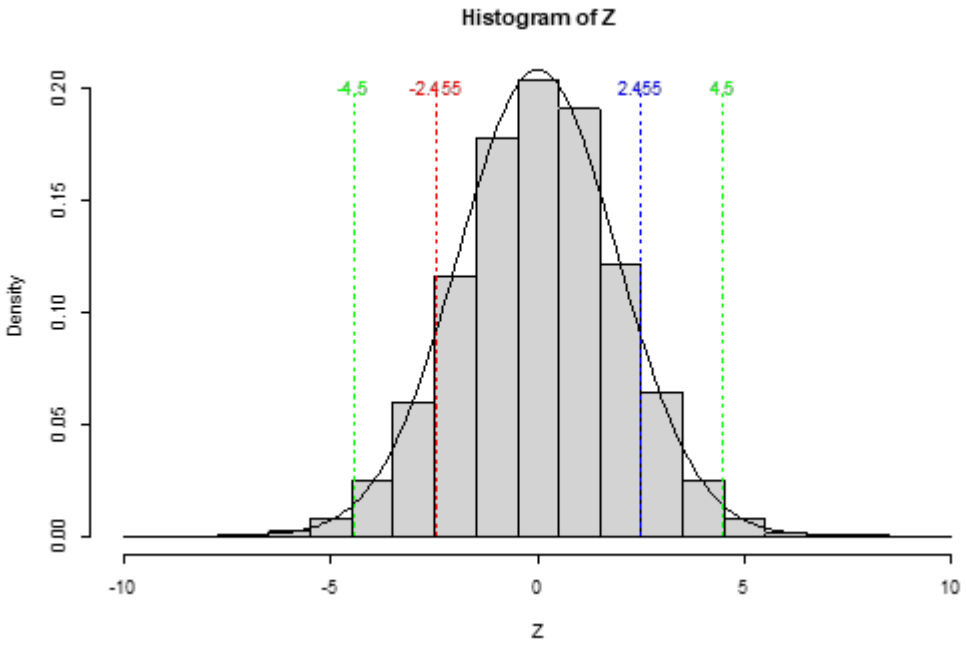

Supplementary Fig. 26. Normal distribution of heat tolerance with a standard deviation of 1.91 and equivalent heat tolerance classes between with $|HT_{max}|$= 8ºC-week.

Cross generational heritability of heat tolerance

Individual colonies are assigned a given heat tolerance class and remain within this class for their entire life from eggs to mature adult. We model transmission of the phenotypic trait of heat

tolerance to the next generation such that it is a trait that is selected for. To achieve this, larvae are allocated to a heat tolerance class with the same approach as per the coral adults.

This is achieved via a vector that describes the proportion of the total larvae at any given site and year within each heat tolerance class (L). This is calculated as:

$$L_t = L_{t-1} + R$$

with *R* being the transgenerational response to selection like the one used in the Breeder's equation[36,63]. We modified the Breeder's equation to allow adjustment of the true distribution of the heat tolerance of the offspring, rather than calculating the mean of a presumed normal distribution, as per the traditional implementation of the Breeder's equation. This allows us to retain the true distribution of the heat tolerance independent of normality, and in addition does not force any assumption about the variance around the mean.

In our implementation, *R* is expressed as a vector rather than a single value containing the proportion of larvae in each heat tolerance class. The generational response is:

$$\overline{R} = h^2 \overline{S}$$

where h^2 is the narrow-sense heritability and *S* is the selection differential also expressed as a vector.

Narrow-sense heritability expresses how much of the trait is transmissible and ranges from 0 (no genetic transmission between parent and offspring) to 1 (100% of the trait is transmitted). Narrow-sense heritability has been investigated in many populations of organisms, and while differences are found, it tends towards $h^2 = 0.3$ for polygenic traits that are non-morphological and related to fitness[64] and therefore we have used this value.

The selection differential is the difference in the distribution of heat tolerances before and after selection pressure is applied (i.e. at the beginning and end of an annual timestep). The selection differential is calculated as:

$$S = L_p - L_{t-1}$$

where L_p is the provisional heat tolerance distribution of this year's larvae calculated from N_t after all selection events of the year have occurred assuming perfect heritability ($h^2 = 1$).

Acknowledgements

The version of the C~scape metacommunity model used here benefitted conceptually and functionally from input from J. Gilmour, M. Gonzalez-Rivero, D. Barneche, B. Robson, K. Crossman, M. Puotinen, J. Moore and the RRAP Modelling & Decision Support team. Parameterising coral demography for the C~scape model simulations was done using the extensive datasets generated by the EcoRRAP subprogram of RRAP: in particular we thank R. Ferrari, C. Doropoulos, M. Toor, S. Gordon and M. Lechene for providing these datasets.

References in Supplementary Information

1. Bozec, Y.-M. *et al.* Cumulative impacts across Australia's Great Barrier Reef: A mechanistic evaluation. *Ecol. Monogr.* **e01494**, (2022).
2. Hock, K., Doropoulos, C., Gorton, R., Condie, S. A. & Mumby, P. J. Split spawning increases robustness of coral larval supply and inter-reef connectivity. *Nat. Commun.* **10**, 3463 (2019).
3. Hock, K. *et al.* Connectivity and systemic resilience of the Great Barrier Reef. *PLoS Biol.* **15**, e2003355 (2017).
4. Herzfeld, M. *et al. eReefs Marine Modelling: Final Report*. 497 pp. http://www.marine.csiro.au/cem/gbr4/eReefs_Marine_Modelling.pdf (2016).
5. Baird, M. E. *et al.* CSIRO Environmental Modelling Suite (EMS): scientific description of the optical and biogeochemical models (vB3p0). *Geosci. Model Dev.* **13**, 4503–4553 (2020).
6. Puotinen, M., Maynard, J. A., Beeden, R., Radford, B. & Williams, G. J. A robust operational model for predicting where tropical cyclone waves damage coral reefs. *Sci. Rep.* **6**, 26009 (2016).
7. Bureau of Meteorology. Australian Tropical Cyclone Database. (2024).
8. Wolff, N. H. *et al.* Temporal clustering of tropical cyclones on the Great Barrier Reef and its ecological importance. *Coral Reefs* **35**, 613–623 (2016).
9. Skirving, W. *et al.* CoralTemp and the coral reef watch coral bleaching heat stress product suite version 3.1. *Remote Sens.* **12**, 3856 (2020).
10. Baird, A. H. *et al.* A decline in bleaching suggests that depth can provide a refuge from global warming in most coral taxa. *Mar. Ecol. Prog. Ser.* **603**, 257–264 (2018).
11. Hughes, T. P. *et al.* Global warming transforms coral reef assemblages. *Nature* **556**, 492 (2018).
12. Humanes, A. *et al.* Within-population variability in coral heat tolerance indicates climate adaptation potential. *Proc. R. Soc. B* **289**, 20220872 (2022).
13. Australian Institute of Marine Science. AIMS-LTMP and MMP Coral Reef Monitoring Modelled Output. https://doi.org/10.25845/q40d-7a72 (2021).
14. Sherwood, S. C. *et al.* An assessment of Earth's climate sensitivity using multiple lines of evidence. *Rev. Geophys.* **58**, e2019RG000678 (2020).
15. Tokarska, K. B., Hegerl, G. C., Schurer, A. P., Forster, P. M. & Marvel, K. Observational constraints on the effective climate sensitivity from the historical period. *Environ. Res. Lett.* **15**, 034043 (2020).
16. Nijsse, F. J., Cox, P. M. & Williamson, M. S. Emergent constraints on transient climate response (TCR) and equilibrium climate sensitivity (ECS) from historical warming in CMIP5 and CMIP6 models. *Earth Syst. Dyn.* **11**, 737–750 (2020).
17. Grose, M. R. *et al.* A CMIP6-based multi-model downscaling ensemble to underpin climate change services in Australia. *Clim. Serv.* **30**, 100368 (2023).
18. Séférian, R. *et al.* Evaluation of CNRM Earth system model, CNRM-ESM2-1: Role of Earth system processes in present-day and future climate. *J. Adv. Model. Earth Syst.* **11**, 4182–4227 (2019).
19. Döscher, R. *et al.* The EC-earth3 Earth system model for the climate model intercomparison project 6. *Geosci. Model Dev. Discuss.* **2021**, 1–90 (2021).
20. Boucher, O. *et al.* Presentation and evaluation of the IPSL-CM6A-LR climate model. *J. Adv. Model. Earth Syst.* **12**, e2019MS002010 (2020).
21. Yukimoto, S. *et al.* The Meteorological Research Institute Earth System Model version 2.0, MRI-ESM2. 0: Description and basic evaluation of the physical component. *J. Meteorol. Soc. Jpn. Ser II* **97**, 931–965 (2019).
22. Sellar, A. A. *et al.* Implementation of UK Earth system models for CMIP6. *J. Adv. Model. Earth Syst.* **12**, e2019MS001946 (2020).

23. Dunne, J. P. *et al.* The GFDL Earth System Model version 4.1 (GFDL-ESM 4.1): Overall coupled model description and simulation characteristics. *J. Adv. Model. Earth Syst.* **12**, e2019MS002015 (2020).
24. Hajima, T. *et al.* Development of the MIROC-ES2L Earth system model and the evaluation of biogeochemical processes and feedbacks. *Geosci. Model Dev.* **13**, 2197–2244 (2020).
25. Müller, W. A. *et al.* A higher-resolution version of the max planck institute earth system model (MPI-ESM1. 2-HR). *J. Adv. Model. Earth Syst.* **10**, 1383–1413 (2018).
26. Tatebe, H. *et al.* Description and basic evaluation of simulated mean state, internal variability, and climate sensitivity in MIROC6. *Geosci. Model Dev.* **12**, 2727–2765 (2019).
27. Seland, Ø. *et al.* Overview of the Norwegian Earth System Model (NorESM2) and key climate response of CMIP6 DECK, historical, and scenario simulations. *Geosci. Model Dev.* **13**, 6165–6200 (2020).
28. Hall, V. & Hughes, T. Reproductive strategies of modular organisms: comparative studies of reef-building corals. *Ecology* **77**, 950–963 (1996).
29. Oliver, J. & Babcock, R. Aspects of the fertilization ecology of broadcast spawning corals: sperm dilution effects and in situ measurements of fertilization. *Biol. Bull.* **183**, 409–417 (1992).
30. Anthony, K. R. Coral reefs under climate change and ocean acidification: challenges and opportunities for management and policy. *Annu. Rev. Environ. Resour.* **41**, 59–81 (2016).
31. Albright, R. Reviewing the effects of ocean acidification on sexual reproduction and early life history stages of reef-building corals. *J. Mar. Sci.* **2011**, 473615 (2011).
32. Doropoulos, C., Ward, S., Diaz-Pulido, G., Hoegh-Guldberg, O. & Mumby, P. J. Ocean acidification reduces coral recruitment by disrupting intimate larval-algal settlement interactions. *Ecol. Lett.* **15**, 338–346 (2012).
33. Byrne, M. *et al.* Catastrophic bleaching in protected reefs of the Southern Great Barrier Reef. *Limnol. Oceanogr. Lett.* (2025).
34. Gilmour, J. P., Smith, L. D., Heyward, A. J., Baird, A. H. & Pratchett, M. S. Recovery of an isolated coral reef system following severe disturbance. *Science* **340**, 69–71 (2013).
35. Pemberton, J. M. Evolution of quantitative traits in the wild: mind the ecology. *Philos. Trans. R. Soc. B Biol. Sci.* **365**, 2431–2438 (2010).
36. Lynch, M. & Walsh, B. *Genetics and Analysis of Quantitative Traits*. vol. 1 (Sinauer Sunderland, MA, 1998).
37. Catullo, R. A., Llewelyn, J., Phillips, B. L. & Moritz, C. C. The potential for rapid evolution under anthropogenic climate change. *Curr. Biol.* **29**, R996–R1007 (2019).
38. Fox, R. J., Donelson, J. M., Schunter, C., Ravasi, T. & Gaitán-Espitia, J. D. *Beyond Buying Time: The Role of Plasticity in Phenotypic Adaptation to Rapid Environmental Change*. *Philosophical transactions of the Royal Society B* vol. 374 20180174 (The Royal Society, 2019).
39. Cornwell, B. *et al.* Widespread variation in heat tolerance and symbiont load are associated with growth tradeoffs in the coral Acropora hyacinthus in Palau. *Elife* **10**, e64790 (2021).
40. Roik, A. *et al.* Trade-offs in a reef-building coral after six years of thermal acclimation. *Sci. Total Environ.* **949**, 174589 (2024).
41. Richards, T. J. *et al.* Moving beyond heritability in the search for coral adaptive potential. *Glob. Change Biol.* **29**, 3869–3882 (2023).
42. Visscher, P. M., Hill, W. G. & Wray, N. R. Heritability in the genomics era-concepts and misconceptions. *Nat. Rev. Genet.* **9**, 255–266 (2008).
43. Howells, E. J. *et al.* Coral thermal tolerance shaped by local adaptation of photosymbionts. *Nat. Clim. Change* **2**, 116–120 (2012).
44. Logan, C. A., Dunne, J. P., Ryan, J. S., Baskett, M. L. & Donner, S. D. Quantifying global potential for coral evolutionary response to climate change. *Nat. Clim. Change* **11**, 537–542 (2021).

45. Sun, C. *et al.* Climate refugia in the Great Barrier Reef may endure into the future. *Sci. Adv.* **10**, eado6884 (2024).
46. Figueiredo, J. *et al.* Global warming decreases connectivity among coral populations. *Nat. Clim. Change* **12**, 83–87 (2022).
47. Great Barrier Reef Marine Park Authority. Great Barrier Reef (GBR) Features (Reef boundaries, QLD Mainland, Islands, Cays, Rocks and Dry Reefs). (2007).
48. Roelfsema, C. M. *et al.* How Much Shallow Coral Habitat Is There on the Great Barrier Reef? *Remote Sens.* **13**, 4343 (2021).
49. Castro-Sanguino, C. *et al.* Control efforts of crown-of-thorns starfish outbreaks to limit future coral decline across the Great Barrier Reef. *Ecosphere* **14**, e4580 (2023).
50. Cresswell, A. K. *et al.* Capturing fine-scale coral dynamics with a metacommunity modelling framework. Sci. Rep. 14, 24733 (2024).
51. Merow, C. *et al.* Advancing population ecology with integral projection models: a practical guide. *Methods Ecol. Evol.* **5**, 99–110 (2014).
52. Kennedy, E. V. *et al.* Reef Cover, a coral reef classification for global habitat mapping from remote sensing. *Sci. Data* **8**, 196 (2021).
53. R Core Team. R: A language and environment for statistical computing. R Foundation for Statistical Computing (2021).
54. Callaghan, D. P., Leon, J. X. & Saunders, M. I. Wave modelling as a proxy for seagrass ecological modelling: Comparing fetch and process-based predictions for a bay and reef lagoon. *Estuar. Coast. Shelf Sci.* **153**, 108–120 (2015).
55. Graham, E. M., Baird, A. H. & Connolly, S. R. Survival dynamics of scleractinian coral larvae and implications for dispersal. *Coral Reefs* **27**, 529–539 (2008).
56. Wallace, C. C. Seasonal peaks and annual fluctuations in recruitment of juvenile scleractinian corals. *Mar. Ecol. Prog. Ser.* 289–298 (1985).
57. Edwards, A. J. *et al.* Direct seeding of mass-cultured coral larvae is not an effective option for reef rehabilitation. *Mar. Ecol. Prog. Ser.* **525**, 105–116 (2015).
58. dela Cruz, D. W. & Harrison, P. L. Enhanced larval supply and recruitment can replenish reef corals on degraded reefs. *Sci. Rep.* **7**, (2017).
59. Doropoulos, C., Elzinga, J., ter Hofstede, R., van Koningsveld, M. & Babcock, R. C. Optimizing industrial-scale coral reef restoration: comparing harvesting wild coral spawn slicks and transplanting gravid adult colonies. *Restor. Ecol.* **27**, 758–767 (2019).
60. Thompson, A. A. & Dolman, A. M. Coral bleaching: one disturbance too many for near-shore reefs of the Great Barrier Reef. *Coral Reefs* **29**, 637–648 (2010).
61. Simpson, M. J. *et al.* Profile likelihood-based parameter and predictive interval analysis guides model choice for ecological population dynamics. *Math. Biosci.* **355**, 108950 (2023).
62. Steven, A. D. *et al.* eReefs: An operational information system for managing the Great Barrier Reef. *J. Oper. Oceanogr.* **12**, S12–S28 (2019).
63. Falconer, D. & Mackay, T. *Introduction to Quantitative Genetics*. (Longman, New York).
64. Moore, M. P., Whiteman, H. H. & Martin, R. A. A mother's legacy: the strength of maternal effects in animal populations. *Ecol. Lett.* **22**, 1620–1628 (2019).